ACIBADEM MEHMET ALI AYDINLAR UNIVERSITY
INSTITUTE OF HEALTH SCIENCES

GENERATION OF HYDROPHOBIN COATED LIPOSOME FOR IMPROVED DRUG BIOAVAILABILITY

FATMA HANDE OSMANAĞAOĞLU

PH.D. THESIS

DEPARTMENT OF MEDICAL BIOTECHNOLOGY

SUPERVISOR
Prof. Meltem Müftüoğlu

SECONDARY SUPERVISOR
Prof. Günseli Bayram Akçapınar

ISTANBUL-2025

ACIBADEM MEHMET ALI AYDINLAR UNIVERSITY
INSTITUTE OF HEALTH SCIENCES

GENERATION OF HYDROPHOBIN COATED LIPOSOME FOR IMPROVED DRUG BIOAVAILABILITY

FATMA HANDE OSMANAĞAOĞLU

PH.D. THESIS

DEPARTMENT OF MEDICAL BIOTECHNOLOGY

SUPERVISOR
Prof. Meltem Müftüoğlu

SECONDARY SUPERVISOR
Prof. Günseli Bayram Akçapınar

ISTANBUL-2025

DECLARATION

I declare that this thesis work is my own work, I had no unethical behavior at any stages from the planning to the writing of the thesis, I obtained all the information in this thesis in accordance with academic and ethicel rules, I cited all the information and comments that were not obtained with this thesis work, and I provided resources in the list of references. I also declare that there was no violation of any patents and copyrights during the study and writing of this thesis.

15/01/2025

"Fatma Hande Osmanağaoğlu"

PREFACE AND ACKNOWLEDGEMENT

This study is an integrated PhD program thesis of Acıbadem Mehmet Ali Aydınlar University Institute of Health Sciences. The aim of the study is to improve bioavailability of low soluble agents with Hydrophobin4 coated liposome delivery system.

I would firstly thank my dear thesis advisor Prof. Meltem Müftüoğlu, who generously shared her knowledge in lab and helped me in each step of this work with full patience and kindness. She is my main motivator to finalize this work. It was a real privilege to work with her.

I would like to thank my second advisor Prof. Günseli Bayram Akçapınar, who introduced me to the fungal world and taught me the essences of lab from scratch with patience generously.

I would like to thank the valuable members of the thesis for their contribution and support.

I am grateful to my dear lab colleagues Busel Özcan, Nedim Can Çevik, Arda Örçen and Ayşegül Ekmekçioğlu, who guided me in lab and encouraged me throughout my PhD journey.

Lastly, I would like to thank my love Tayfun Osmanağaoğlu and my dear mother Şekbal Türçak for their valuable support and motivation during the thesis. Without their help, it would not be possible to finalize the thesis.

I dedicate this work to my father by realizing his will and proposal and my precious children Ziya Arda Osmanağaoğlu and Alp Tuna Osmanağaoğlu hoping to show them nothing is impossible and there is no limit for new beginnings in life.

TABLE OF CONTENTS

ABBREVIATIONS AND SYMBOLS

BMG	Buffered glycerol complex
BMM	Buffered methanol complex
Dox	Doxorubicin
Dox-HFB4L	Doxorubicin loaded hydrophobin coated liposome
Dox-PPL	Doxorubicin loaded PEG coated liposome
Gr	Gram
GRAVY	Grand average of hydropathicity
H	Hour
HFB	Hydrophobin
HFB4L	Hydrophobin coated liposome
HFB4	Hydrophobin4
LB	Luria Bertani
Min	Minute
Mg	Miligram
Ml	Mililiter
MCF7	Human breast cancer cell line with estrogen, progesterone and glucocorticoid receptors
Nm	Nanometer
NP	Nanoparticle
PEG	Polyethylene glycol
PPL	PEG coated liposome
Rpm	Round per minute
S	Second
SDS-PAGE	Sodium-dodecyl sulphate agarose gel electrophoresis
YNB	Yeast nitrogen base
YPD	Yeast extract peptone dextrose agar

LIST OF FIGURES

LIST OF TABLES

ABSTRACT

Generation of Hydrophobin Coated Liposome for Improved Drug Bioavailability

The surface properties of nanoparticles are vital in determining how they interact with biological environments, affecting factors such as cellular uptake, targeting capabilities, stability and biocompatibility. Hydrophobin 4 (HFB4), a class II hydrophobin derived from filamentous fungi, naturally self-assembles at hydrophobic-hydrophilic interfaces. Due to its biocompatibility, non-toxicity, biodegradability, and amphipathic nature, HFB4 is particularly beneficial for enhancing the solubility and bioavailability of water-insoluble agents. This study examined and compared the physicochemical properties (including size, polydispersity index, zeta potential, morphology, stability, and release rate at various pH levels), as well as internalization to cell and antitumor efficacy of both HFB4-coated empty liposomes (HFB4L) and Doxorubicin-loaded liposomes (Dox-HFB4L) to PEGylated liposomes (PPL). All formulations have a good size homogeneity, spherical, and homogenous morphology. Encapsulation with HFB4 enhanced the stability for Dox-HFB4L over 60 days at 4 °C while not significantly impacting the release of Dox HFB4L. Additionally, it facilitated a higher release of Dox at acidic pH (pH 5.6) in comparison to to physiological pH (pH 7.4), suggesting the delivery of hydrophobic drugs to low pH tumor environments. Both formulations demonstrated higher cellular uptake than free Dox, but they had a reduced antitumor effect because of the controlled release of Dox. Importantly, Dox-HFB4L exhibited higher cytotoxicity than Dox-PPL in MCF7 cells. It can be proposed that coating liposomes with HFB4 might provide enhanced advantages for delivering water-insoluble drugs to tumor cells and tissues in a sustained, stable and non-toxic way.

Keywords: Hydrophobin 4 (HFB4), Liposome, Doxorubicin, Drug delivery, Nanoparticles

ÖZET

İlaç Biyoyararlımının Arttırılması İçin Hidrofobin Kaplı Lipozom Geliştirilmesi

Nanoparçacıkların yüzey özellikleri, biyolojik çevresi ile etkileşimi yanında, kararlılığı, biyouyumluluğu, hedefleme kabiliyeti ve hücre içine alımında da kritik etkisi bulunmaktadır. Hidrofobin4 (HFB4) ipliksi mantarlar tarafından üretilen bir sınıf II hidrofobin proteini olup, hidrofobik-hidrofilik arayüzde doğal olarak dizilme özelliğine sahiptir. HFB4 biyouyumluğu, toksik olmaması, biyolojik olarak parçalanabilmesi ve amfipatik olması gibi değerli özellikleri, hidrofobik ilaçların çözünürlüğü ve biyoyararlanımın arttırılmasında potansiyel fayda sağlayabilir. Bu çalışmada, HFB4 kaplı doksorubisin içeren lipozomun fizyokimyasal özellikleri (büyüklük, çoklu dağılım endeksi, zeta potansiyeli, morfoljisi, kararlılığı ve farklı pH değerlerinde ilaç salınımı), hücre içine alımı ve antikanser etkileri araştırılmış olup PEG kaplı lipozom ile karşılaştırılmıştır. Araştırma sonucunda bütün formülasyonların küresel olup, büyüklük ve morfoloji açısından iyi bir homojenliğe sahip olduğu gözlemlenmiştir, 4 °C derecede 60 gün süren çalışmada, HFB4 kaplamasının ilaç salınım profilini değiştirmeden lipozomun fizyokimyasal kararlılığını arttırdığını göstermiştir. Ayrıca asidik pH'ta (pH 5.6) fizyolojik pH'a (pH 7.4) göre daha yüksek doksorubisin salınımı sağlaması sebebiyle, hidrofobik ilaçların asidik tümör ortamına dağıtımında avantaj sağlaması beklenmektedir. Benzer özellikler doksorubisin yüklü PEG kaplı lipozomda da gözlemlenmiştir. Her iki formülasyon ile konvansiyonel doksorubisine göre daha yüksek hücre içine alım gösterilmiş olup anti-kanser etkinin uzun salınım etkisi sebebiyle daha düşük olduğu gözlemlenmiştir. MCF7 kanser hücre hattı üzerinde doksorubisin ile yapılan çalışmada HFB4 kaplı lipozomun, PEG kaplı lipozoma göre daha yüksek sitotoksisite sağladığı görülmüştür. Bu sonuçlar doğrultusunda, lipozom kaplamasında HFB4 kullanımının hidrofobik ilaçları toksik olmayan, kararlılığını koruyan, ve uzatmalı salınım sağlayacak şekilde tümör ortamına taşınmasında yüksek fayda sağlayacağı gösterilmiştir.

Anahtar Sözcükler: Hidrofobin4 (HFB4), Lipozom, Doksorubisin, İlaç taşıma, Nanoparçacıklar.

1 INTRODUCTION AND AIM

Altering nanoparticle outer layer with proteins can facilitate their durability, targeting abilities, biocompatibility, and internalization, making it an effective strategy for developing sophisticated drug delivery systems (1, 2). The surface features of nanoparticles can have an impact on their interplay with biological systems, their directing ability to target cells, their existence in blood circulation and ability to escape from immune system. The cellular level it can influence the interaction of nanoparticles with cells and their uptake capability, which is crucial for therapeutic efficacy. Increased stability and biocompatibility in the biological ecosystem with protein-modified nanoparticles can help minimizing the drug related toxicity and enhance the pharmacological outline (3-8). Hydrophobins (HFBs) can modify surfaces of nanoparticles, and provide potential benefits for biomedical applications (9, 10).

Hydrophobin 4 (HFB4) is a product of filamentous fungi and it is a member of class II HFB proteins. HFB4 can self-assemble at hydrophobic-hydrophilic boundary into amphipathic layers and can alter the hydrophilic-hydrophobic nature of the outer layer, like other HFBs (11). This relatively stable and approximately 10 nm thin layer of HFB protein offer a convenient way for reverse the outer layer characteristics, protein adsorption, biodistribution, and modification (4, 12, 13). The amphipathic property of HFBs makes them beneficial for enhancing the hydrophobic drugs solubility and consequently their bioavailability. It is seen that the HFB coating of airborne fungal spores is responsible for prevention of immune recognition. So, HFBs also contribute the avert of immune reaction (14). This HFB coating can be applied to liposomes to protect against the *in vivo* immune organization and avert its response. Furthermore, the non-toxicity, biocompatibility, and biodegradability of HFBs render them ideal for drug delivery systems (15, 16). In the literature HFBs have been studied for directly coating of drugs (10, 17-21) and also coating the drug-carrying nanoparticles surfaces (4, 5). It was shown that HFB coating stabilized drug nanocrystals and improved the bioavailability of water-insoluble agents (17), and provided sustained and directed drug delivery through surface alteration (18, 19).

PEG-covered liposomal Dox, Doxil® which was developed to address the dose-limiting toxicity associated with conventional Dox therapy and has been available since 1995 (22). The creation of stealth liposomes through the surface covering with polyethylene glycol (PEG) is employed to prolong the half-life of liposomes in the blood circulation (23). PEGylation can diminish protein adsorption and as a result it can impart a stealth effect. However, it can also influence the plasma proteins that attach to the carrier, resulting in lowered internalization versus non-coated carriers (5, 24). The PEGylation can also restrict cellular interplay with directed cells and their absorption (25-27). Anti-PEG antibodies found in human body can disturb the membrane unity and lead to the burst release of enclosed Dox from the PEGylated liposome (PPL), which opposes with hiddenness effect of PEGylation (28).

HFBs may be preferred as an option to widely used PEG for altering the surface properties of nanocarriers; potentially providing numerous advantages in terms of biocompatibility, stability, and drug delivery performance.

The purpose of this work is to generate HFB4-coated empty (HFB4L), and Dox-loaded liposomes (Dox-HFB4L) and assess their physicochemical properties and antitumor impact on breast cancer cell line MCF7 and compare the findings with those of PEGylated liposomes (PPL).

There is no study reported in the literature on hydrophobin coating of liposomes for drug delivery. This study is unique in terms of modifying the drug carrier liposome surface with the fungal protein HFB and offer a new drug delivery option for hydrophobic drugs.

2 BACKGROUND

2.1 Liposomes as Drug Carriers

The newly developed drugs offer new solutions to the diseases however most of them are poorly water-soluble and, they often exhibit poor bioavailability. To overcome this problem different methods have been developed but still there is a demand for improvement for better drug delivery systems, especially using nanotechnology. Polymeric nanocarriers and lipid nanocarriers developed for this aim are examples of this effort and these systems are now widely used (18).

Liposomes, the lipid nanocarriers, are spherical, small, self-sealing arrangements with one or multiple concentric lipid bilayers encapsulating a hydrous phase in the center. Phospholipids are the primary component of liposomes. They have an amphiphilic nature, featuring a hydrophobic tail and hydrophilic head. The hydrophilic component primarily consists of phosphoric acid attached to a water-dissolvable molecule, while the water-insoluble portion is composed of two fatty acid chains containing 10-24 carbon atoms and 0-6 double bonds per chain. Phospholipids generate lamellar sheets in aqueous medium by orienting themselves so that the charged head face outwards towards the hydrous phase, while the fatty acid groups facade inward, generating a spherical, vesicular framework known as liposomes. The charged part stays in touch with the hydrous part while the uncharged part is shielded. If phospholipids are dispersed in aqueous media, the application of energy through methods such as sonication, shaking or heating leads to hydrophilic and hydrophobic interactions between lipid-lipid and lipid-water molecules. These interactions result in the formation of bilayered vesicles, facilitating the achievement of thermodynamic equilibrium in the liquid part. Their self-assembly, emulsifying characteristics and wetting properties are all attributed to their amphipathicity. If phospholipids are hydrated, they spontaneously organize, producing various frameworks with distinct specifications under different conditions.

Phospholipids naturally tend to generate liposomes, which may be utilized as drug directing agents. They also possess excellent emulsifying properties that help steady emulsions. Moreover, their wetting characteristics can be applied for coating hydrophobic drugs to enhance their hydrophilicity. These three attributes are integral to various drug design studies. Variations in aliphatic chains and alcohols result in the formation of diverse phospholipids, and different origin of phospholipids contribute to this diversity (29).

Liposomes can be evaluated according to their scale and quantity of bilayers. They are categorized as multilamellar vesicles (MLV), large unilamellar vesicles (LUV) and small unilamellar vesicles (SUV). Based on their content, they can be assessed as immuno-liposomes, pH-sensitive liposomes, long circulating liposomes (LCL) cationic liposomes, and conventional liposomes (CL). Additionally, liposomes can be also organized according to their preparation method, including ether injection vesicles (EIV), reverse phase evaporation vesicles (REV), and French press vesicles (FPV) (29).

A liposome comprised of a hydrous solution enclosed within a hydrophobic membrane. Hydrophobic materials can be easily dissolved in the lipid layers, facilitating liposomes to convey both hydrophobic and hydrophilic agents. The specific position of the drug within the liposome will rely on its physiochemical properties and the lipid mix. To deliver essential chemicals to the target site, the lipid bilayers merge with the cell membrane, facilitating release of the chemical content (29).

The process of liposome-mediated drug delivery involves several steps: first, liposomes adsorb onto the cell layer membrane, followed by their immersion and adsorption. Next, the lipid bilayers of the liposomes merge with the lipoidal cell membrane through lateral diffusion and lipid intermingling, leading to the direct release of the liposomal contents into the cytoplasm. Phospholipids, being the primary components of cell membranes, provide excellent biocompatibility due to their amphiphilic properties. The membrane of liposomes resembles the cell membranes, due to lipid content, lipid transfer proteins readily identify liposomes and facilitate lipid interchange. For instance, in tumor cells, which require a big amount of lipid for rapid

proliferation, they identify drug loaded liposomes as a possible source of nutrients. Once the anti-tumor substance are discharged from the liposome at that point, they effectively kill the cancer cells (29).

Benefits of using liposomes as a drug distribution method for antimicrobials include improved management over pharmacological properties, reduced toxicity, enhanced drug effectiveness against intracellular pathogens, targeted selectivity, and increased activity against cellular pathogens (29).

As advantages explained, liposomes have been extensively utilized as drug distribution mean since their invention, thanks to their biocompatible and biodegradable properties, as well as their special ability to carry hydrophilic agents in the hydrous core and water-insoluble drugs within the lipid bilayers. This versatility makes them effective therapeutic transporters (23). Liposomal drug delivery provides substantial therapeutic advantages for poorly soluble compounds.

In current formulations of anticancer agents, solubilizers such as organic co-solvents and various surfactants are used in formulation to improve solubility, however these solubilizers can lead to toxicity at the doses administered. At present, liposomes are employed as excipients to create better accepted clinical design for various lipophilic and sparingly water-dissolvable agents (30).

Although liposomes have various advantages, there are also some shortcomings during their application such as stability problems, limited shelf life, low encapsulation efficiency and quick elimination from blood-circulation by immune system (29).

The generation of stealth liposomes involves applying a surface revision of a hydrophilic polymer, typically a lipid by-product of polyethylene glycol (PEG), to prolong the half-life in blood circulation (23). Currently, the standard method for minimizing unspecific internalization of drug delivery agents is through the covalent attachment of PEG. It is believed that PEG can diminish protein integration, thus

creating a hiddenness effect. However, it may also alter the mix of plasma proteins that attach to the carrier, resulting in lower internalization versus non-coated carriers (5, 24).

The PEG moiety creates an aqueous layer on the surface of liposomes, stabilizing the lipid bilayer and providing steric hindrance, which inhibits protein adsorption and reduces recognition by macrophages. The term "stealth" is used to describe these liposomes due to their ability to evade detection by the immune system, like how a stealth bomber avoids radar detection. The PEGylated liposomal delivery system allows for long-term circulation and accumulation in cancerous tissue via enhanced permeation and retention (EPR). However, the aqueous layer created by the PEG moiety hinders the interaction of the liposomal delivery system with the target cell surface, leading to minimal or no cellular uptake. Additionally, PEGylation enhances the steadiness of the lipid packaging, which results in ineffective endosomal evade through membrane merge and disintegration of cargoes in lysosomes, the cell's digestive compartments. The PEG surface can restrict cellular interactions and internalization with target cells. These significant challenges associated with PEG use are known as the “PEG dilemma”(26, 27).

As explained earlier, the surface properties of nanocarriers influence not only the stability of the particles and drug release profile but also their internalization by cells, their existence in circulation, their distribution in various tissues, and their interactions with proteins, cells, tissues, or organs. Ultimately, these factors dictate the fate of nanocarriers in the body following administration (4). Due to the nature of the liposomes and PEG dilemma, there is still room for further improvement in this area. Therefore, other surface-active molecules such as hydrophobins could form robust alternatives to PEG by changing the surface characteristics of nanocarriers.

2.2 Hydrophobins and Their Use in Drug Delivery

Hydrophobins (HFBs) are soluble proteins produced by fungi that spontaneously organize into an amphipathic membrane when they encounter a boundary (such as air - cell wall). These proteins have been linked to various aspects of fungal development.

For instance, the self-assembly of HFBs is believed to contribute to the constitution of hyphae and fruiting bodies. Arrangement at the air-medium boundary reduces surface strain, enabling hyphae to penetrate the medium–air boundary. Spontaneously organization at the air-cell-wall boundary creates a water-repellent layer that coats aerial hyphae and air branches in fruiting bodies. HFBs also play a role in the attachment of hyphae to hydrophobic layers; for instance, over the course of symbiotic or pathogenic relationship, a layer was constructed by self-assembly of HFBs.

The assembled HFBs have different stability profiles based on their solubility and amphipathy, allowing for the distinction of at least two classes of HFBs. Class I HFBs create very insoluble assemblies that can only be liquefied in highly acidic materials, such as formic or trifluoroacetic acid. In contrast, Class II HFBs can be liquified by applying pressure or decreasing the temperature, or by putting in ethanol or sodium dodecyl sulfate. Besides eight cysteine residues forming disulfide bridges with consistent spacing, HFB sequences are not highly conserved. Generally, Class I HFBs consist of 100–125 amino acids and may be glycosylated, while Class II HFBs are shorter, formulated by 50–100 amino acid. Class I HFBs have been found in Basidiomycetes and Ascomycetes. Class II HFBs have only been identified in Ascomycetes. It is observed that Class I HFB network display higher β-sheet structure compared to the soluble form, a trend not seen in Class II HFBs. Furthermore, a link has been established between the β-sheet structures and the steadiness of the assemblies (31).

HFBs can alter the hydrophilic-hydrophobic nature of an outer layer by self-assembling into a very narrow and relatively steady monolayer of 10 nm. This offers a practical method for modifying surface physicochemical characteristics, protein attachment, and delivery (4). With this specification, HFBs provide an option to PEG for modifying the surface properties of nano sized vehicles.

The ability of HFBs to self-assemble into stable structures enables their use in numerous applications including drug delivery, stability, and controlled release. Their amphipathic property provides valuable means for enhancing the dissolvability and

bioavailability of hydrophobic agents. Additionally, HFBs are biocompatible, non-toxic, and biodegradable, making them suitable for drug delivery systems. It is shown that HFB inhibits detection by immune system of fungal spores, thereby contributing to the prevention of the immune response against these spores (14). The HFB4 coating on the liposome raises the hypothesis that these proteins may provide a shield against immune-system and thereby preventing the action of immune system.

HFBs have been utilized either to directly coat the drug (10, 17-20) or to cover the outer layer of the drug carrying nano vehicles (4, 5).

It was shown that HFBs enhance the water-insoluble agents bioavailability by steadying drug nanocrystals through direct coating with the class I HFB SC3 of *Schizophyllum commune* (17). In another research, direct coating of an anti-cancer agent docetaxel with class I HFB protein H star Protein B showed reduced burst release, but study results were not supported with cytotoxicity and stability data of the new formulation (18). The study to generate class I HFB recombinant HGFI (rHGFI) coated curcumin nanoparticles showed better cytotoxicity profile, meets the nanomeric size need and have a favorable release profile than uncoated curcumin. However, the low drug loading level seems still a drawback and there is no information on stability of new formulation (19). Another study done with curcumin and rHGFI provides only 96 h stability results, with supporting better antitumor activity supported with in vitro and in vivo studies (20). Class II HFBs were also utilized for drug coating, targeting nanomeric size and increasing solubility of the hydrophobic drug beclomethasone dipropionate with coating HFBII (10).

HFBs were also utilized for coating drug nanoparticles such as polylactic-co-glycolic acid (PLGA) and niasome. Coating curcumin loaded PLGA nanoparticles with class I HFB protein H star Protein B showed higher effect on cancer cells but increased systemic and liver toxicity (4). Development of niasomal nano-formulation coated with class I HFBI for cancer inhibition showed higher encapsulation efficiency and better sustained profile compared to PEG coating, with reduced cytotoxic effect with coating either with PEG or HFB (5).

The only research in the literature on HFB4 is coating drug free porous silicon nanoparticles (Psi) with plant-produced transferrin-HFB fusion protein. The new formulation shows safer profile in terms of toxicity in breast cancer up to 150 μM/mL dose, but its stability, drug release, and effectiveness should be further studied (6).

2.3 Doxorubicin in Cancer Treatment

Among chemotherapeutic agents, Dox is one of the most thoroughly studied one in relation to drug-distribution methods (22).

Originally derived from the natural pigment daunorubicin, which is produced by various strains of Streptomyces, daunorubicin was isolated and developed into an antibiotic effective against tumors. This compound was successfully used to treat acute leukemia and lymphoma, but by 1967, it became clear that daunorubicin cause severe toxicity of cardio. To address this issue, researchers genetically modified Streptomyces species to create Adriamycin, now known as doxorubicin. Doxorubicin is a 14-hydroxylated derivative of daunorubicin, and although it has a higher therapeutic index, its cardiotoxicity remains a significant concern (32).

Doxorubicin exerts its effect by interposing with DNA, thereby hindering molecular synthesis and interfering with the enzyme topoisomerase II, which is crucial for DNA relaxation during transcription. When doxorubicin stabilizes the topoisomerase II complex after the DNA chain has been splitted for replication, it prevents the refastening of the DNA double helix, halting replication. Additionally, doxorubicin generates free radicals that can damage DNA and cell membranes (32).

This drug is primarily used to treat various cancers, including those of the, breast, thyroid, stomach, soft tissue sarcoma, bladder, lung, multiple myeloma, ovaries, and Hodgkin’s lymphoma. The cardiotoxicity of conventional doxorubicin poses a major challenge during treatment, often limiting its dosage (32).

To enhance the safety profile of traditional anthracyclines, numerous strategies have been developed. These include creating novel anthracycline analogs, employing low-dose continuous infusion schedules, co-administering with the cardioprotective agent dexrazoxane, and utilizing liposomal encapsulation technology. The primary dose-limiting toxicity of doxorubicin is cardiomyopathy, which can cause congestive heart failure and potentially fatal outcomes. One effective strategy to mitigate doxorubicin-related toxicity is the use of drug carriers that alter the pharmacological distribution of the drug, thereby reducing its concentration in the heart. Liposomal formulations, in particular, have proven to be the most successful approach to improving the therapeutic index of conventional anthracyclines (32).

Myocet® and Doxil® are liposomal forms of Dox in the market, which are developed to cope with the dose-limiting toxicity of conventional Dox.

Pegated liposomal doxorubicins, including Doxil®, can lead to dose-limiting hand-foot syndrome (HFS). This condition is marked by skin rashes on the hand and/or foot, which often requires a treatment interruption of at least two weeks and a subsequent dosage reduction of 25%. This syndrome has been reported in nearly 50% of patients treated with a dose of 50 mg/m², according to the Doxil Product Information leaflet. Although Doxil® (pegylated liposomal doxorubicin) exhibits a strong affinity for the skin and has an extended circulation time, a significant drawback is the occurrence of dose-limiting HFS (32).

Nonylated liposomal doxorubicin Myocet® offers a safer alternative compared to both conventional doxorubicin and Doxil®. However, the high cost of Myocet® has limited its widespread adoption. Additionally, its administration is complicated by the requirement of a three-vial system. Given established efficacy and safety profiles, future studies will ideally focus on evaluating the treatment costs associated with the novel liposomal doxorubicin formulations to determine their potential for widespread use and effectiveness in treating cancer patients (32).

2.4 Other Methods Used for Effective Doxorubicin Delivery

Among new formulations, only liposomal doxorubicin has been thoroughly researched and evaluated in clinical trials involving patients with various stages of cancer. The other formulations are mainly organic nanocarriers, protein based nanocarriers, micelles, supramolecules and hydrogels.

Polymeric nanoparticles serve as organic nanocarriers made up of biocompatible, and frequently biodegradable materials at nano size. They are simple, soft materials due to their synthesis and ease of structural revision. This enables the incorporation of specific properties into the nanoparticles, such as outer layer revision that enhance drug loading efficiency, biodistribution, pharmacological management, and effectiveness (33, 34).

Polymeric nanoparticles can be constructed from synthetic polymers, such as poly(lactic acid) (PLA) and poly(styrene-maleic anhydride) copolymer, or from natural polymers like chitosan, gelatin, collagen and dextran. Drugs are efficiently packaged by either dispersing them within the polymer matrix or attaching them to polymer material for prolonged delivery.

Synthetic polymers offer the benefit of prolonged drug release that can extend from days to several weeks, unlike natural polymers, which typically provide a shorter release duration. Additionally, synthetic polymers allow for utilization of organic solvents and have specific conditions required during the encapsulation process. As result, polymeric nanoparticles are extensively studied as drug distribution vehicles, including PLA and PLGA nanoparticles.

Dox was attached with dextran and then packaged in a hydrogel utilizing a reverse microemulsion method to diminish its toxic effects and augment its efficacy in handling tumor tissues (35).

Albumin is one of the preferred agents for protein based-nanocarriers. It can be sourced from various origins, including egg whites, human serum, bovine serum, as well as from milk, grains and soybeans. Album-based nanocarriers offer numerous advantages, including straightforward preparation, high drug binding capacity, nontoxicity, non-immunogenicity, biocompatibility, and biodegradability, along with a prolonged circulation time. The functional groups on the surfaces of albumin nano vehicles facilitates the surface modifications (36).

Doxorubicine-loaded human serum albumin (HSA) nano vehicles, as an example for protein based nanocarrier, have demonstrated superior antitumor efficacy in in vitro study compared to the pure drug when tested in neuroblastoma (37).

Micelles are spherical colloidal nanosized carriers created through the spontaneous organization of amphiphilic copolymers in a watery solution, which results in surrounding of water-insoluble core surrounded by a water-dissolved hydrophilic shell. The nucleus acts as a repository for water insoluble agents, while the hydrophilic shell secure the nucleus and enhances the water solubility of both the polymer and the water insoluble materials, turning the vehicle a suitable alternative for intravenous administration. The incorporation of drugs into a micelle occurs through electrostatic interactions, chemical or physical interactions (23).

Doxorubicin is packed into cationic 1,2-dioleoyl-3-trimethylammonium propane/methoxy polyethyleneglycol (DPP) nanoparticle, forming micelles to deliver Dox to vesical, and has demonstrated an antitumor effect to bladder tumor (38).

Supramolecules, as a drug carrier, are composed of multiple molecular units held together by frail and convertible noncovalent interactions, including electrostatic forces, hydrogen bonds and van der Waals forces. As a result, they are anticipated to serve as carriers in drug distribution systems. Supramolecular systems can act as means for covering and delivering therapeutic agents or bioactive materials in a targeted manner (23).

Systemic toxicity of conventional antitumor drugs, like doxorubicin, can be mitigated by using amphiphilic dendrimers that form supramolecular micelles for cancer treatment (39). Supramolecular polymersomes encapsulating Dox demonstrate extended circulation, and better efficacy against HeLa cells with safer toxicity profile (40).

Hydrogels are three-dimensional hydrophilic and polymeric structures that can take up significant quantities of biological materials. Hydrogels are extensively utilized in various applications within therapeutic and diagnostic fields, such as artificial skin, linings for artificial hearts and biosensors. Additionally, they can be employed for three-dimensional cell growth and as drug distribution agents (23). Hydrogels are effective options for sustained release, or directed drug distribution because they can pack biological molecules, as well as hydrophilic or hydrophobic drugs (41).

Doxorubicin loaded poly(methacrylic acid) (PMAA) hydrogel can achieve cellular decomposition and acid-base sensitiveness by incorporating cystamine crosslinks (42). The attachment protocol during the early stage of internalization is significantly influenced by the morphology of the particles, with hydrogel spheres demonstrating 12% superior toxic effect compared to cubes for 10 hours when tested on HeLa cells.

Poly(vinylcaprolactam) (PVCL)-based microgels to encapsulate Dox have been generated for stimulis-activated discharge in low pH environments (43). DOX carrying microgels demonstrate higher efficacy against HeLa line versus empty microgels (44).

The goal of the study is to improve delivery of hydrophobic and/or poor water-soluble pharmaceutical agents to cells, such as water-insoluble chemotherapeutic agents to cancer cells with liposome carrier system, which is stabilized with HFB rather than conventional PEG. The effect of HFB coating of liposome on entrapment efficiency of drug, *in vitro* drug release, effect on cancer cell viability and cellular uptake and stability will be evaluated with the model drug doxorubicin. Results will be compared with lean liposome and PEG-coated liposome.

3 MATERIALS AND METHODS

3.1 Materials

Pichia pastoris KM71H and *E.coli* DH5α strains were from Thermofisher, USA. Cholesterol, L-α-Phosphatidylcholine from egg yolk (L-α-PC), and phosphate buffer saline (PBS) tablets, lithium acetate dihydrate and biotin were purchased from Sigma-Aldrich (USA). 1,2-distearoyl-sn-glycero-3-phosphoethanolamine-N-[methoxy(polyethyleneglycol)-2000] (ammonium salt) (18:0 PEG2000 PE, PEG) was from Avanti-Polar lipids (USA). Dichloromethane (DCM), sodium acetate trihydrate ($CH_3COONa \cdot 3H_2O$), sodium sulfate (Na_2SO_4), acetic acid (glacial), potassium dihydrogen phosphate, and di-potassium hydrogen phosphate, and ammonium sulfate were products of Merck (Germany). Dulbecco's phosphate-buffered saline (DPBS), SYBR Safe-DNA Gel Stain, SACI enzyme, Penicillin/Streptomycin (Pen/Strep), Zeocin, 1-Step™ NBT/BCIP Substrate, 6x-His Tag Monoclonal Antibody (3D5), AP, Pierce Silver Stain Kit and Pierce BCA Protein Assay Kit were obtained from Thermo Scientific (USA). The dry regenerated cellulose dialysis membrane (MWCO: 10 kDa, 30 mm flat width) was purchased from CelluSep (USA). Uranyl acetate was supplied from Electron Microscopy Sciences (USA). Dox was purchased from Santa Cruz Biotechnology (USA). Fetal bovine serum (FBS) and Dulbecco's modified eagle medium (DMEM) were from Gibco (USA). The SRB assay kit was supplied from Abcam (UK). The MCF7 cell line was from the American Type Culture Collection (ATCC, USA). Tween-80, Yeast Extract Peptone Dextrose Medium (YPD), Laura-Bertani Medium, and Yeast Nitrogen Base (YNB) without amino acids and ammonium sulfate were supplied from Research Products International (RPI, USA). Qiaprep Spin Miniprep Kit was purchased from Qiagen (USA). Methanol and glycerol were purchased from Isolab (Germany). Genomic DNA Clean and Concentrator 25 was purchased from Zymo Research (USA).

Devices used in the thesis were all present in Acibadem Mehmet Ali Aydinlar University Research and Development Laboratory as listed in Table 1.

Table 1. Devices used in the production and analysis.

Device type	**Device Name**
Angled centrifuge	Beckman Coulter-Allegra 64R
Elecroporator	Biorad Genepulser Xcell
Elisa Reader	Thermo Varioscan Flash
Fluorescent microscope	Zeiss AX10
Flow Cytometry	BD FACSVerse Flow Cytometry
Freeze-Dryer	Labconco Freezone 6 Plus
Gel imaging system	Biorad Chemidoc MP
Microbiology cabinet	Safe-2020
Microplate spectrophotometer	Powerwave XS2 BioTek
Mini centrifuge	Thermo MicroCL17
Multi rotator	Biosan MultiBioRS-24
Nanodrop	Thermo Nanodrop One C
Particle Size and Zeta Potential Measurement	Anton Paar LiteSizer 500
Rotary Evaporator	Stuart RE300
Thermal Cycler	Biorad T100
Thermomixer heater	Eppendorf Thermomixer Comfort
Transmission electron microscope	Thermo Scientific Talos L120C
Ultracentrifuge	Beckman Coulter Optima Max-XP
Ultrasound	Bandelin Sonorex GT 1003 M-C
Western Blot semi-dry system	Biorad Transblot Turbo

Table 2. Stock solutions used in the production and characterization studies.

Stock Solution and Buffer	**Recipe**
Low Salt Luria Bertani Broth (LB)	20 grams (gr) LB broth is dissolved in 1000 ml ddH_2O and autoclaved at 121 °C for 15 minutes (min).
Low Salt Luria Bertani Agar with Zeocin	35 gr LB agar is dissolved in 1000 ml ddH_2O and autoclaved at 121 °C for 15 min. 25 µg/ml Zeocin (Invitrogen) was added when the solution cool to 55°C and transferred to the petri dishes.
Yeast Extract Peptone Dextrose Broth (YPD)	50 gr YPD agar is dissolved in 1000 ml ddH_2O and autoclaved at 121°C for 15 min.
Yeast Extract Peptone Dextrose Agar (YPD) with Zeocin	65 gr YPD agar is dissolved in 1000 ml ddH_2O and autoclaved at 121°C for 15 min at 121°C. 100 µg/ml Zeocin (Invitrogen) was added when solution cools to 55°C, transferred to petri dishes.
10X Yeast Nitrogen Base (YNB) (without Ammonium sulphate and amino acids)	100 gr ammonium sulphate and 34 grYNB are dissolved in 1000 ml ddH_2O. Sterilized by filtering and stored at 4°C.
BMM (Buffered Methanol Complex) Agar	4 gr agar and 138 ml of ddH_2O are autoclaved at 121°C for 15 min. 20 ml potassium phosphate buffer at pH 6, 20 ml 10X methanol, 20 ml 10X YNB, 400 µl 500X Biotin are added and transferred to the petri dishes.
500X Biotin (0.02% Biotin)	20 mg biotin is dissolved in 100 ml of ddH_2. Sterilized by filtering and stored at 4°C.
10X Methanol (5% Methanol)	5 ml methanol is mixed with 95 ml ddH_2O. Sterilized by filtering and stored at 4°C.
10X Glycerol	10 ml glycerol is mixed with 90 ml ddH_2O and then autoclaved at 121°C for 15 min.
1000X CuSO4 (0.5 M CuSO4)	7.98 gr CuSO4 is dissolved in 100 ml of ddH_2O. Sterilized by filtering and stored at 4°C.

Table 2. Stock solutions used in the production and characterization studies (continued).

Stock Solution and Buffer	**Recipe**
1 M Potassium Phosphate Buffer (pH: 6)	868 ml 1 M KH_2PO_4 and 132 ml 1 M K_2HPO_4 are mixed, and pH was adjusted by adding 1 M KOH.
1X Buffered Glycerol Complex Media (BMGY)	100 ml 10X YNB, 100 ml 10X Glycerol, 100 ml 1 M Potassium phosphate buffer at pH 6.0, 2 ml 500X Biotin and 698 ml sterile ddH_2O are mixed under sterile conditions and stored at 4°C.
1X Buffered Methanol Complex Media (BMMY)	100 ml of 10X YNB, 100 ml 10X Methanol, 100 ml 1 M Potassium phosphate buffer at pH 6.0, 2 ml 500X Biotin and 698 ml sterile ddH_2O were mixed under sterile conditions and stored at 4°C.
Super Optimal Broth (SOB)	28 gr SOB is dissolved in 1000 ml ddH_2O and sterilized by autoclaving at 121 °C for 15 min.
Super Optimal Broth with Catabolite repression (SOC)	28 gr SOB is dissolved in 1000 ml ddH_2O and sterilized by autoclaving at 121 °C for 15 min. 20 ml 1 M glucose is added after the solution is cooled down and sterilized by filtering with 0.22 µm filter.
10X Tris- Borate-EDTA (TBE) Buffer	55 gr Boric acid and 108 gr Tris base are dissolved in 900 ml ddH_2O. 40 ml 0.5 M Na_2EDTA (pH:8.0) is added and volume is adjusted to 1000 ml.
10X SDS-PAGE Running Buffer	144 gr glycine (1.92 M), 30 gr Tris base (0.25 M), 10 gr Sodium dodecyl sulphate (SDS) (0.03 M) mixed in 800 ml ddH_2O, volume adjusted 1000 ml.
Tris-HCL 0.5 M (pH:6.8)	6 gr Tris base is dissolved in 70 ml ddH_2O. pH is adjusted to 6.8 with HCl. Finally, volume is adjusted to 100 ml.
Tris-HCL 1.5 M (pH:8.8)	18 gr Tris base is dissolved in 70 ml of ddH_2O. pH is adjusted to 8.8 with HCl. Finally, volume is adjusted to 100 ml.

Table 2. Stock solutions used in the production and characterization studies (continued).

Stock Solution and Buffer	**Recipe**
2X Urea Sample Buffer	4.8 ml Tris-HCl, 16 ml of 10% SDS, 9.6 gr urea, 8 ml glycerol and 40 miligram (mg) bromophenol blue are mixed in 40 ml ddH_2O.
10% SDS	10 gr SDS is dissolved in 100 ml ddH_2O and sterilized by filtering.
Towbin Transfer Buffer	14 gr (192 mM) glycine and 3 gr (25 mM) Tris base are mixed.
10X Tris-Buffered Saline (TBS) Solution	88 gr NaCl and 24 gr Tris base are dissolved in 900 ml ddH_2O. pH is adjusted to 7.6 with 12N HCl. Volume is adjusted to 1000 ml.
10X Tris-Buffered Saline with Tween 20 (TBS-T)	400 µl (0.5%) Tween-20 is added into the TBS solution and mixed.

3.2 Bioinformatics Analysis

HFB 1, HFB 2 from *Trichoderma reesei* and HFB 4 from *Trichoderma virens* core HFB regions were used in analysis. Protein sequences were used to calculate protein physiochemical properties with EXPASY ProtParam web tool. (https://web.expasy.org/protparam/) (45).

Clustal ω was employed to determine multiple sequence alignment of the core HFB region for the HFBs HFBI, HFBII and HFB4 (46). MView was used to calculate the consensus sequences (46).

3.3 Production and Purification of HFB4

The HFB4 expression, generation, and purification in *Pichia pastoris* KM71H strain (Invitrogen) were conducted in line with Invitrogen EasySelect ™ Pichia Expression Kit user manual.

A codon-optimized synthetic HFB4 gene encoding a 65 amino acid core HFB region (Uniprot ID: A0A7D5LY27) was cloned to the pPICZαA vector between the *EcoRI-XbaI* sites in Figure 1. (47)

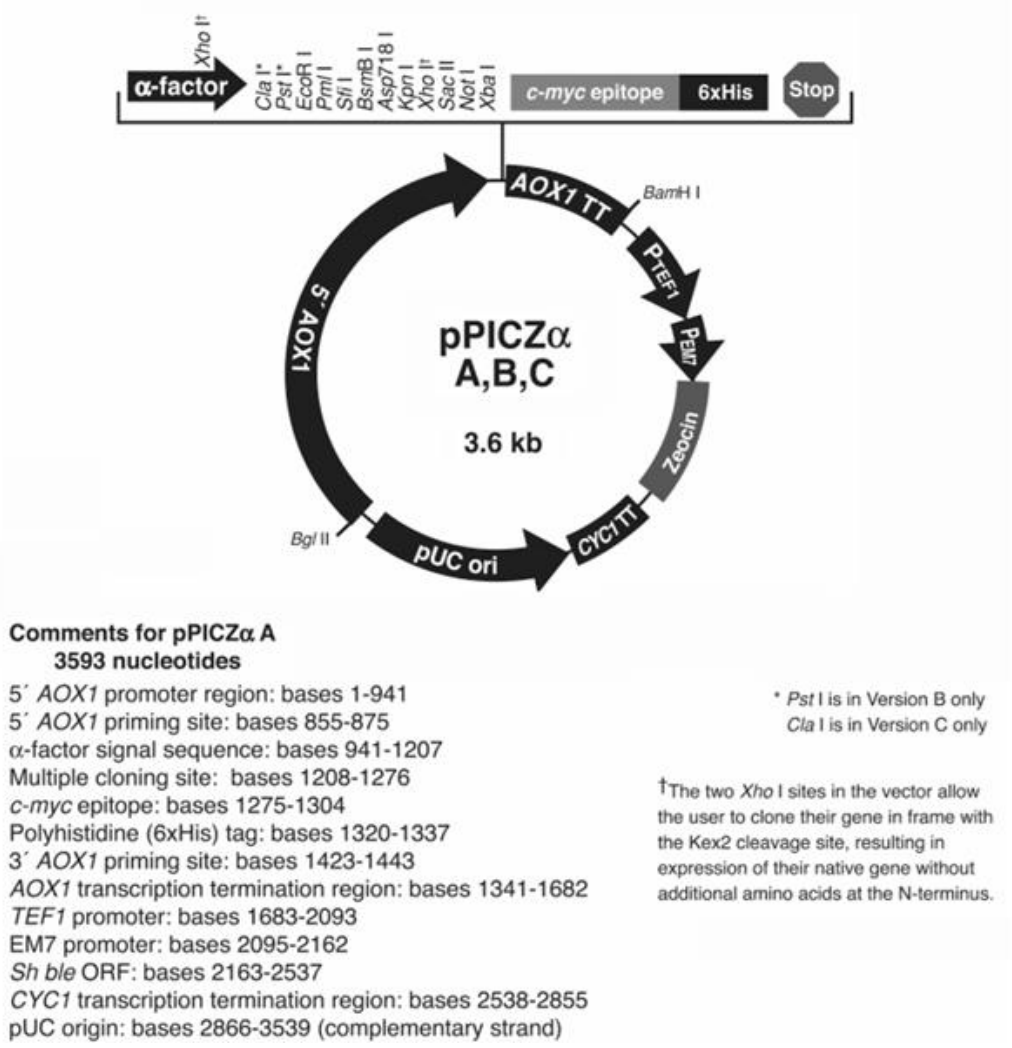

Figure 1. pPICZαA vector used in the cloning step.

The vector with the synthetic construct was transformed into competent *E.coli* DH5α cells by applying the heat shock method. For this aim, 50 µl competent cell was

added to 1 µl HFB4 containing plasmid and kept on ice for 45 min. This mixture is then treated with heat for 90 seconds (s) at 42 ºC in Eppendorf Thermomixer Comfort. Following the heat treatment, the mixture is kept on ice for 2 min and afterwards 880 µl SOC was added. To allow expression of antibiotic resistance genes, the mixture was put to shaker for 2 h at 37 ºC and 150 rpm. 50 µl of transformant was seeded on LB agar plate having 25 µg/ml Zeocin. Plates were covered to protect from light and grown at 37 ºC throughout the night.

A recombinant plasmid containing the synthetic HFB4 was refined by using the mini prep (Qiagen Plasmid Mini Prep Kit) following the manufacturer's protocol. For this aim, a colony taken from LB agar was put into 5 ml liquid LB medium and incubated overnight in shaker at 37 ºC at 150 rpm. The next day, 1 ml of bacterial culture was spinned at 6800 x g for 3 min at room temperature. The pelleted cells were redispersed in 250 µl Buffer-P1 from the Mini Prep Kit and placed to a microcentrifuge tube. Next, 250 µl Buffer-P2 was put and mixed until the solution becomes clear. Then 350 µl of Buffer-N3 was added, blended and centrifuged at 17 900 x g for 10 min. The mixture was then put into QIAprep spin column and spinned for 60 s. The flow-through was disposed and the column was cleaned with 0.5 ml Buffer-PB 60 s with centrifugation. The washing step was iterated with 0.75 ml Buffer-PE. Finaly the column was put in a clean microcentrifuge tube and DNA was extracted from the column by placing 50 µl Buffer-EB and centrifuge for 1 min. The eluted DNA is then measured at Thermo Scientific Nanodrop One Microvolume Spectrophotometer.

To linearize the plasmid, 7.5 µl of elute containing 3 µgr DNA was added to 18.5 µl water and 3 µl buffer. Then 1 ml *SacI* enzyme was put and spinned at 13 200 rpm for 30 s. The mixture was treated at heat-block overnight at 37 ºC. The following day DNA cleaning and concentration step was applied with Zymo Research DNA Clean and Concentrator Kit. First 60 µl of DNA binding buffer was put to the mixture and blended with vortexing. Then mixture was relocated in collection tube to Zymo-spin column and spinned for 30 s. The flowthrough was disposed and 200 µl DNA wash buffer was placed to column. After centrifugation the flowthrough was discarded, and

this wash step was iterated. Finally, 10 µl DNA elution buffer was put to column matrix, let for incubation 5 min than placed to 1.5 ml tube for centrifugation for 30 s.

The following step was transfer of cleaned and concentrated HFB4 DNA to chemically competent *Pichia pastoris* through electroporation method (48). For this aim, 3 µg of plasmids were put on component KM71H cells on ice and incubated for 5 min. Then samples were placed in a 2 mm electroporation cuvette and incubated again for 5 min. Electroporation was done at Biorad Gene Pulser Xcell at 1.5 kV, 25 µF and 25 Ohm. After electroporation 1 M ice-cold sorbitol was added and samples were transferred to Eppendorf tubes for incubation at 30 ºC for 2 hours (h). Following the incubation, 100 µl of sample was spread with glass beads to YPD agar plates with 100 µg/ml Zeocin. The plate was grown at 30 ºC for 72 h. The selection of transformants were performed on YPD agar plates with 100 µgr/ml Zeocin. The existence of HFB4 gene was verified with colony PCR using AOX primers 5'AOX (5'- GACTGGTTCCAATTGACAAGC-3') and 3' AOX (3' AOX: 5' GCAAATGGCATTCTGACATCC-3'). Samples taken from different parts of the YPD plate were put on Eppendorf tubes and treated with heat at microwave for two min. Then samples were put on ice and 50 µl double distilled water was added. PCR mixture was prepared in PCR tubes with adding each 0.5 µl 10 mM 5' AOX and 3' AOX primers, 5 µl 2X TaqPCR Master Mix and 3 µl double distilled water on template DNA. PCR was done at Thermal Cycler Biorad T100 with 5 min initial denaturation step at 94 ºC and 30 s denaturation step at 95 ºC, followed by 34 cycles of 1 min annealing at 54 ºC and 1 min extension at 72 ºC, completed with 10 min extension at 72 ºC. Verification was completed with electrophoresis at 100 V for 1 h on 1.2% agarose gel containing 10,000X Invitrogen SYBR Green Safe dye. Selected colonies were streaked to the YPD Zeocin 100 µgr/ml agar plates and replated three times to confirm single colony.

Expression optimization was performed with expression in 96-deep well plate to select best productive transformant. Eight colonies from different points of agar plate were put into 5 ml YPD broths and incubated in the shaker incubator at 30 ºC 180 rpm overnight. Samples were checked under light microscope against contamination and

pellets were retrieved by centrifugation at 5 000 rpm 5 min. The pellets were dissolved at 2X BMG media and transferred to the wells and put to shaker incubator at 30 ºC 180 rpm overnight. The following day OD_{600} of the samples were measured with Thermo Nanodrop One C with diluting the samples 1/50. The amount accounting for 60 OD were collected with centrifugation and dissolved in 2 ml 2X BMM media. For each colony duplicate samples of cells in BMM medium were put into wells of 96-deep well plates containing sterile glass beads. At the starting point and following 24 h and 48 h 50 µl of sample was collected and 20.8 µl of 20 % filtered methanol was added to induce protein expression. These analysis samples were centrifuged to separate protein containing supernatants from cell pellets and stored at -20 ºC until analysis. After 48 h samples were collected and supernatants and pellets were retrieved with centrifugation at 5 000 rpm for 10 min.

The highest production capacity colony was selected according to optical density measured with Thermo Pierce Protein BCA Assay kit. The microplate procedure of the manual has been applied while preparing the standards and test samples. 1X BMM and ddH_2O were used as blank and measurements were done with Thermo Flash device at 562 nm. BCA assay result was confirmed with SDS-PAGE electrophoresis method. For this aim 4% Stacking gel and 16 % resolving gel was prepared according to Biorad Handcasting Polyacrylamide Gel manual. Samples were prepared by mixing protein containing supernatant 1:1 with 2X urea sample buffer with B-mercaptoethanol and treating with heat at 95 ºC for 5 min. 20 µl sample was loaded to the gels with and run under 100 Volt for 2 h. PageRuler Prestained protein ladder was used to determine molecular weight of proteins in the gel. Thermo Pierce Silver Stain Kit was applied to visualize electrophoresis results with Chemidoc MP. The colony with highest protein production capacity determined with BCA Assay and confirmed SDS PAGE electrophoresis result was selected to express the protein at high amounts at baffled shake flasks.

For this aim the colony taken with a pipette tip was put into 100 ml YPD broth in 500 ml baffled flasks and incubated at 30 ºC 180 rpm for two days. Before transfer to BMG medium samples from all flasks were examined with light microscope against

contamination. Then cell pellets were collected with ultracentrifuge at 5000 rpm 5 min and dissolved in 100 ml 1X BMG media for incubation overnight at 30 ºC 180 rpm. The following day again samples were analyzed under microscope and after confirming the sterile conditions, OD_{600} of samples in baffled flasks were measured. The amount corresponding to 60 OD (final 30 OD/ml) were centrifuged to separate cells from supernatant and dissolved in 100 ml 1X BMM media. 1 ml sample was collected for analysis, centrifuged to separate pellet from supernatant and stored at -20 ºC until analysis. Flasks were incubated in the shaker for 48 h at 30 ºC 180 rpm and 1 ml samples were taken for analysis every 24 h. The flask contents were kept constant by adding 1 ml 100% filtered methanol after taking 1 ml sample for analysis.

Supernatant was separated after 48-h expression process with applying centrifuge and stored at +4 ºC. The recombinant HFB4 was purified through multiple ultrafiltration steps. The supernatant of production step was concentrated and buffer was exchanged with PBS with a 10kDa cut-off ultrafiltration cassette (Sartorius, Vivaspin 6, 10 kDa MWCO PES) followed by ultrafiltration through a 30 kDa ultrafiltration cassette (Merck Millipore, Amicon Ultra Centrifugal Filter, 30 kDa MWCO, regenerated cellulose) to eliminate higher molecular weight proteins. With this two-step ultrafiltration, HFB4 protein identified as a dimer at 13 kDa was separated from other proteins in the supernatant.

Pierce bicinchoninic acid (BCA) micro-plate procedure was used to determine the protein concentrations. HFB4's existence in the purified solution was confirmed with SDS PAGE protocol as applied in production optimization process.

For Western blotting, refined HFB4 protein was visualized on 16% SDS-polyacrylamide gels. For determining the molecular weight of proteins PageRuler Prestained Protein Ladder was used in the process. The HFB4 protein in the gel is then transmitted to a polyvinylidene fluoride (PVDF) membrane with semidry transfer method, followed by the blocking step. 5% non-fat dry milk in TBST (10 mM Tris–HCl, pH 8.0, 150 mM NaCl, 0.1% Tween-20) was used for this purpose. The membrane was then incubated with alkaline phosphatase-conjugated mouse 6x-His

Tag monoclonal antibody (dilution ratio 1:1000). Subsequently, the membrane was treated with the One-step NBT/BCIP substrate following the protocol (Pierce). Immunoblots images were taken with ChemiDoc MP Imaging systems (Bio-Rad Laboratories, USA).

3.4 Preparation of Empty and Dox-loaded Liposomes Coated with HFB4 or PEG

Liposomes were generated according to Bangham's thin film hydration method with some modifications as explained in previous studies (1, 21). Empty PEG liposomes (PPL) were generated by blending L-α-PC: cholesterol: PEG in the ratio of 0.92:1.00:0.08 (mole %) according to Table 3.

Table 3. Empty 8% PEG liposome ingredients.

	cholesterol	**L-α-phosphatidylcholine**	**PEG**
% mol	1	0.92	0.08
mg (weight)	6	10.82	3.48
stock (mg/ml)	10	10	10
Added volume µl	600	1082	348

These substances were blended in DCM and then in rotary evaporator lipid film was generated. The excess DCM was discarded overnight using a vacuum desiccator. Next day, the film generated was hydrated by using 4 ml DPBS (at pH 7.4) and incubated through the night at 4 ºC for self-assembly.

HFB4 liposomes (HFB4L) were produced with the same procedure with some modifications. Firstly, L α-PC: cholesterol in the proportion of 0.92:1.00 (mole %) was mixed in DCM, then the thin film was formed with treating rotary evaporator and vacuum desiccator as applied above. After the hydration with DBPS (pH7.4) of the dried lipid film, 1 ml HFB4 solution (10.47 gr lyophilized HFB4 in 1 ml ddH_2O) was put to the solution (final ratio of cholesterol to L-α-PC to HFB4 becomes 1:0.92:0.08)

and the final composition becomes as presented in Table 4. A magnetic stirrer homogenized the mixture at room temperature.

Table 4. Empty 8% HFB4 liposome ingredients.

	cholesterol	**L-α-phosphatidylcholine**	**HFB4**
% mol	1	0.92	0.08
mg (weight)	6	10.82	10.47
stock (mg/ml)	10	10	10
Added volume µl	600	1082	1047

Both liposomal formulations were sonicated 30 min in an ultrasonic bath. Then the mixture was centrifuged at 4 °C, 200 000xg for 16 h to remove any abundant materials. Then the flowthrough was disposed, and the pellet was treated twice with 1 ml sterile dH_2O for washing. The ultimate liposomal formulation was achieved by refining through 0.45 µm filter (Spritzen PES Syringe filter 0.45 µm) followed by filtering through 0.22 µm (Spritzen PES Syringe filter 0.22 µm) filters.

The Dox-loaded HFB4L (Dox-HFB4L) and Dox-loaded PPL (Dox-PPL) were prepared similarly, except for putting 100 µM Dox to the lipid composition before the thin film generation step. Form long term stability, liposomes were freeze-dried and kept in refrigerator lyophilized at 4 °C. Different studies proved that incorporating sucrose as a lyoprotectant before freeze-drying, the liposome stability was improved (49-52). In this study, Sucrose was selected as the lyoprotectant and added to the liposome mixture with a molar ratio:3.1 sucrose-to-lipid before freeze-drying. The freshly prepared liposome samples were aliquoted in Eppendorf tubes and the lyophilization process was performed under -70 °C, 0.1 mbar pressure, 48 h conditions (Labconco, Freezone 6 Plus). For storage the lyophilized samples were kept in refrigerator at 4 °C.

3.5 Characterization of Liposomes

The liposome stability was determined by liquefying the lyophilized liposomes with pure water by shaken by hand for 20 sec and then determining their particle size, polydispersity index, and zeta potential using the dynamic light scattering. For particle size measurement 850 µl sample was put into disposable cuvette (Sarstedt Cuvette Polystyrene 10x10x45 mm) and automatic angle and water was selected as solvent in measurement parameters. The average size of particles was expressed as mean ± standard deviation (n=3).

For zeta potential measurement, samples were prepared by blending 50 µl liposome with 450 µl 1 mM NaCl. Then 350 µl from the mixture was loaded to Anton Paar Omega cuvette. The parameters were determined as Smoluchowski approximation at 25 ºC, automatic 200 V power adjustment, water as solvent and 20 run at manual quality. Measurement was average of 4 serial measurements with a mean and standard deviation.

The liposome morphology was determined by transmission electron microscope (TEM, Talos L120C, Thermo Scientific, USA). For this aim, 10 µl of liposome was put onto the copper grid (LC300-Cu-25 Lacey/Carbon 300 Mesh) and negatively stained with 2% uranyl acetate. 92.000X magnification was applied while investigating the dried sample.

3.6 Encapsulation Efficiency

The coated Dox in Dox-PPL and Dox-HFB4L amount was determined using Varioskan Flash spectral scanning multimode reader (Thermo Scientific, USA). Firstly, a Dox calibration curve (serial concentrations ranging from 2 µM to 20 µM) was constructed at excitation/emission spectra at 470/490-800 nm. 595 nm wavelength was determined as the maximum fluorescence intensity (λmax). The linear line y (RFU) = (conc) x + n equation created from the Dox calibration curve at 595 and used to determine unknown Dox concentration. To measure the concentration of Dox

loaded liposomes, the samples were mixed 1:1 ratio with ethanol and vortexing is applied to release the drug content. Then, the solutions fluorescence was measured at excitation/emission 470/490-800 nm. The unknown Dox concentrations were computed according to the equation y (RFU) = 3.24 (conc) x + 9.35 (R^2= 0.98), where y is the RFU measured at 595 nm. Comparison of the final Dox concentration of the liposome with the Dox concentration used in the preparation step gave the encapsulation efficiency. By multiplying this ratio with 100, the percent encapsulation efficiency was attained.

3.7 In vitro Drug Release

The Dox release from the liposomes were determined at physiological pH (pH 7.4) and acidic environment (pH 5.6). For this aim, a closed dialysis bag (cut-off 10 kDa, CelluSep, USA) filled with 500 µl of drug-loaded liposome was put into 40 ml of citrate buffer (pH 5.6) or PBS buffer (pH 7.4). For each pH a triplicate experiment setup was prepared (n=3). The buffer was shaken at 37 °C and 100 rpm. The samples were harvested for analysis at 15 min, 30 min, 45 min, 1 h, 2 h, 6 h, 12 h 24 h, and 36 h. Release medium volume was kept constant by adding fresh buffer. Dox content in the sample was measured by fluorometric scale at 595 nm using a multimode reader (VarioSkan Flash, Thermo Scientific, USA). A new Dox calibration curve (serial concentrations ranging from 0.1 µM to 0.8 µM and from 0.02 µM to 0.4 µM) was produced at 595 nm since the Dox released to the buffer was 80 times diluted. The total weight and concentration of Dox in the release buffer were computed according to the Dox calibration curve equations; (at pH 7.4) y (RFU) = 6.50 (conc) x + 0.02 (R^2= 0.99) and (at pH 5.6) y (RFU) = 5.31 (conc) x + 0.02 (R^2= 0.99). The released Dox in the media was presented for 36 h as the cumulative release and percent release was determined by taking the weight ratios of cumulative Dox released vs initial Dox at the start of the experiment in the dialysis bag.

3.8 Cellular Uptake of Liposomes

In vitro studies were experimented on MCF7 (human breast adenocarcinoma) cells. The cells were grown in DMEM and augmented with 10% FBS, 1% Pen/Strep and maintained at a incubator humidified 37 °C, 5% CO_2. The cellular uptake of liposomes was analyzed in 6-well plates, where 300 000 cells was seeded in each well with complete DMEM w/o phenol red. The following day, cells were treated with 1 h with 5 μM Dox loaded liposomes, Dox-PPL, and Dox-HFB4L at 37 °C in serum-free DMEM w/o phenol red. Cells were washed twice after the incubation with ice-cold 1X DPBS and cells were collected from the wells by using trypsin. Pellets were collected by centrifugation for 5 min at 600xg then washed twice with ice-cold 1X DPBS and then re-suspended in 400 μl 1X DPBS. The samples were maintained on ice. Cellular uptake of Dox in different formulations was measured with 550 nm laser FACS Caliber flow cytometer (BD FACSVerse flow cytometer). The cells were gated based on forward vs. side scatter to exclude dead cells prior to analysis by FACS, with a total of 10,000 cells counted. PE-A channel was used to analyze the data with BD FACSVerse software.

3.9 In vitro Cytotoxicity of Empty and Dox-loaded Liposomes

The free and liposomal formulation cytotoxicity of Dox was evaluated by using MCF7 cell line with SRB Assay. As preparation, adherent ~80% confluent MCF7 cells were trypsinized and spinned at 600xg for 5 min. Then the cells were dispersed by adding 5 ml DMEM growth medium. The cell density was measured by using a hemocytometer. Appropriate concentration of cells was prepared by adding DMEM and 5 000 cells/well in 200 μL were seeded to clear flat-bottom 96-well plate and put to incubator for 24 h.

The serial dilutions from 0.0625 μM to 1 μM were prepared for empty and drug loaded liposomes by using DMSO as the solvent. DMSO effect was checked before the experiment to eliminate the DMSO impact on cytotoxicity at the maximum concentration in the experiment. Then the seeding medium was removed and 200 μL

of treatment samples were added. Only cell culture medium was put to the control cells. The plate was incubated in a humidified incubator at 37°C for 72 h with 5% CO2. Following this step, 50 µl fixation solution was put to wells and kept at 4 °C for 1 h for incubation. Following the fixation step, the solution was removed gently to protect the cell layer at the bottom of wells and then washed carefully three times with 200 µL dH_2O. After this step the wells were checked against any remnant of dH_2O, and 45 µl of SRB solution was gently injected to dried wells and kept 15 min at a dark place. After incubation, the staining solution was eliminated by pipetting and wells were washed with 200 µL washing solution. This step was repeated four times. Finally, wash solutions were removed quickly by pipetting and 200 µL of 1X solubilization solution was added to wells and allow for mixing by 10 min shaking. Finally, the absorbance was measured at 565 nm. (Powerwave XS2, BioTek, Vermont, USA). IC50 was calculated using the GraphPad Prism.

3.10 Statistical Analysis

All data were expressed as the mean ± STD from three experiments. One-way ANOVA was used for statistical analysis with multiple comparisons, followed by Tukey post-hoc tests. The analysis was performed using the GraphPad Prism 9.2.0 software and a p-value of < 0.05 was considered statistically significant.

4 RESULTS

4.1 Bioinformatic Analysis

HFBI, HFBII and HFB4 physiochemical properties of were presented in Table 5. Due to the closeness of pI to the blood pH, 7.2-7.4, HFB4 was used in thesis study. It is expected that a higher number of positively charged residues may increase the interaction with negatively charged membranes. Also, HFB4 has a similar aliphatic index to HFBII.

Table 5. HFBI, HFBII and HFB4 physiochemical properties. Expasy ProtParam Tool (https://web.expasy.org/protparam/) was used to predict HFBs properties.

	Molecular Weight (kDa)	**Theoretical pI**	**Total number of positively charged residues (Arg + Lys)**	**Instability index**	**Aliphatic Index**	**Grand average of hydropathicity (GRAVY)**
HFBI	6.6	6.0	3.0	29.7	89.8	0.4
HFBII	6.5	5.4	3.0	-1.3	102.2	0.8
HFB4	6.4	8.2	4.0	14.2	97.4	0.5

Consensus sequences and multiple sequence alignment dictate that the hydrophobicity and main HFB Cysteine motifs were well preserved in all three HFBs. Also, consensus analysis and MSA results indicated that the main hydrophobic patch region of all HFBs is well conserved (Figure 2).

Figure 2. Multiple Sequence Alignment of HFBI, HFBII and HFB4 with Clustal Omega. (A) Mview visualization of MSA exhibiting conserved residues (B**).**

4.2 Production and Purification of HFB4

A synthetic and codon-optimized HFB4 gene, which encodes a 65 amino acid core HFB region of HFB4 (Uniprot ID: A0A7D5LY27) was inserted into the pPICZαA vector between the *EcoRI-XbaI* sites. Vectors with the synthetic construct were transferred into competent DH5α of *E.coli* cells with heat shock procedure. Cells were spread via 0.2 mm glass beads on LB agar plates with Zeocin (25 µg/ml). Figure 3 shows Zeocin resistant colonies. Colonies taken from the agar plate were signed as 1 and 2 in the Figure 3.

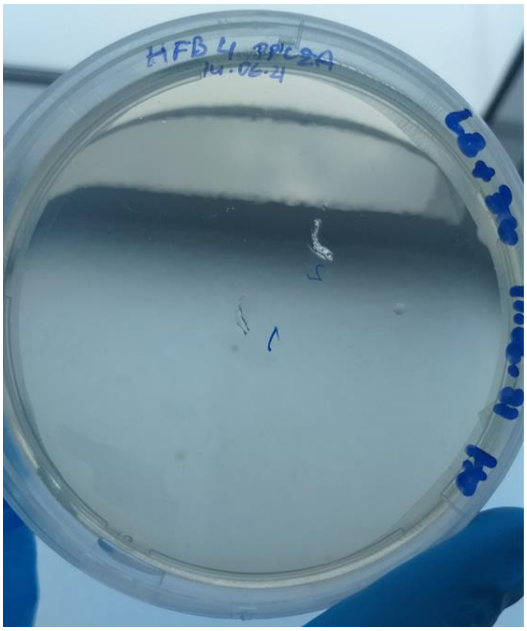

Figure 3. Low salt LB agar (Zeocin 25 µg/ml) *E.coli DH5α* transformation plate for HFB4.

Transformed colonies were cultured in LB broth at 37 °C until plasmid isolation. Qiagen Plasmid Mini Prep kit was used for purification. Concentration of HFB4, A260/280 and A260/230 values were measured with NanoDrop as shown in Table 6. Results showed that the concentration is high, and samples don't have any contaminants.

Table 6. MiniPrep plasmid isolation results.

	Concentration (ng/µl)	A260/280	A260/230
HFB4	416	1.92	2.86

Purified and linearized samples were transformed into *P. pastoris* KM71H competent cells via high efficiency electroporation method. Samples were spread to Zeocin (100 µg/ml) containing YPD agar plates. The resistant colonies, and samples taken for microwave colony PCR verification were shown in Figure 4.

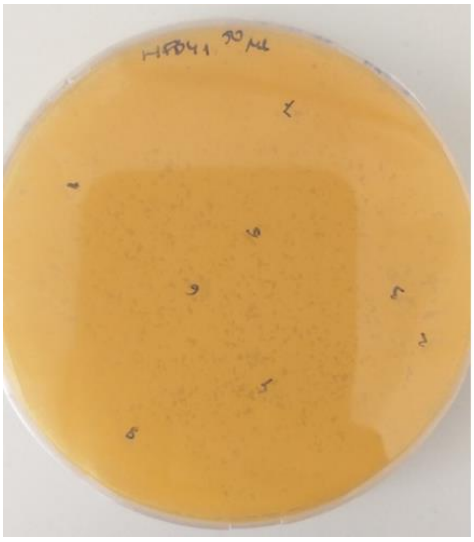

Figure 4. *P.Pastoris* KH71H strain YPD Zeocin (100 µg/ml) transformation master plate.

Positive transformants were checked with microwave colony PCR. Samples were analyzed at 1.2% agarose gel at 100V for 80 min. Empty vector pPICZαA was employed as the positive control and ddH_2O was utilized as the negative control. Samples were transformed successfully according to gel results.

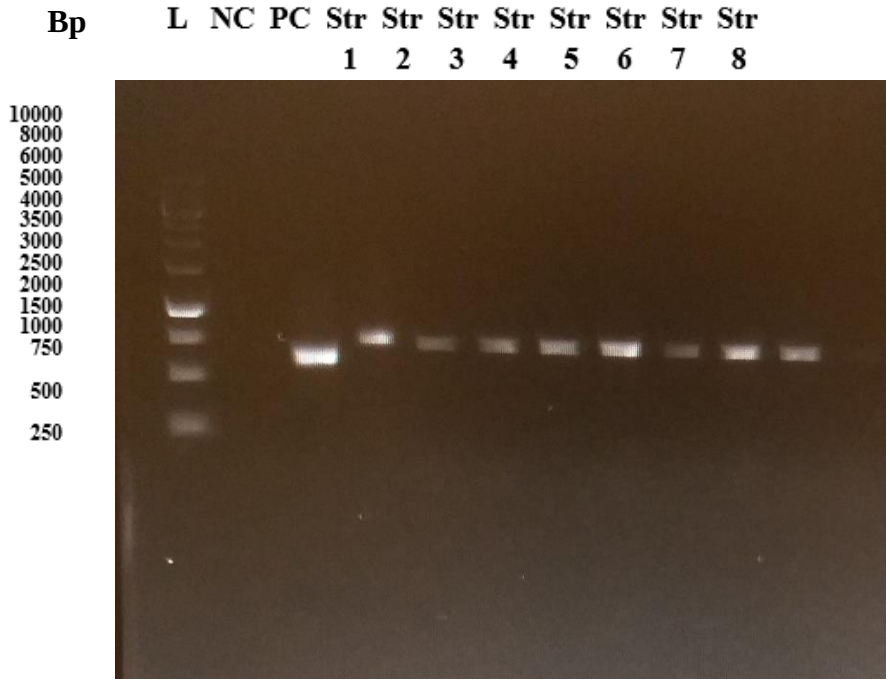

Figure 5. Colony PCR results of 8 colonies of HFB4 (L: Generuler 1kb ladder mix, PC: pPICZα, NC: ddH_2O).

pPICzαA has 588 bp and insertion of HFB4 which is comprised of 65 amino acids will increase the size of the vector. As seen in Figure 5 samples of HFB4 inserted pPICZαA ran slower than empty pPICZα confirming the HFB4 insertions. 8 of positive colonies were selected and streaked to Zeocin (100 µg/ml) YPD agar plates for each sample and grown at 30°C for three days. This step was repeated three times to pure and single colony. (Figure 6)

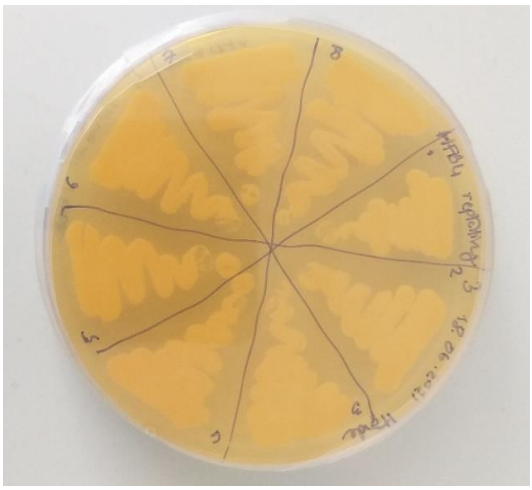

Figure 6. HFB4 colonies after third replating.

Expression optimization was performed with expression in 96-deep well plate to select best productive transformant. Following the growth and production step, production capacity of transformants were measured as given in Table 7.

Table 7. Production optimization study results.

HFB4 Colonies	**OD562 at 24 h**	**OD562 at 48 h**
HFB4 Colony 1	0.04752	0.06651
HFB4 Colony 2	0.05931	0.05394
HFB4 Colony 3	0.04702	0.09337
HFB4 Colony 4	0.02494	0.06416
HFB4 Colony 5	0.02788	0.09462
HFB4 Colony 6	0.01893	0.07064
HFB4 Colony 7	0.02069	0.03433
HFB4 Colony 8	0.03509	0.04328

The highest production capacity colony 5 of HFB was selected according to total protein amount measured and confirmed with SDS PAGE electrophoresis result. This colony was selected to express the protein at high amounts at baffled shake flasks.

Protein containing supernatant in 500 ml baffled flasks were harvested with centrifugation after 48-h expression process. Production of HFB4 was confirmed with SDS gel electrophoresis as shown in Figure 7A. The total protein concentration was measured 223 µgr/ml with BCA Assay. Recombinant HFB4 was purified through a two-step ultrafiltration step as explained in method section. HFB4 determined as a dimer at 13 kDa. This target protein was refined from other proteins in the supernatant as given in Figure 7B and the final purified HFB4 concentration was measured as 43 µg/ml with BCA Assay. Western Blot study confirmed that purified protein is exactly HFB4 in line with previously confirmed immunoblot study (53).

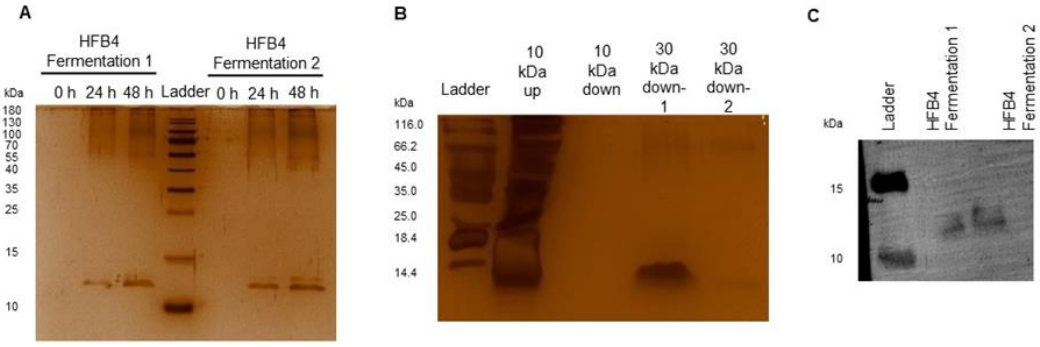

Figure 7. SDS-PAGE verification of HFB4 production (A) SDS-PAGE verification of purification (B) Western Blot of refined HFB4 (C).

4.3 Characterization of Empty and Dox-HFB4L and Dox-PPL

All liposomal formulations average particle size, PDI, and zeta potential are presented in Table 2. The PDI below 0.2 is indicating good size homogeneity for all liposomal formulations (54). It is seen that all liposomal formulations have negative surface charge due to negative zeta potential results. Adding lyoprotectant before lyophilization did not significantly change the liposomes' particle PDI, size and zeta potential ($p>0.05$). The data in Table 4 presents the average and standard deviation of three measurements.

Table 8. Characterization of liposomes.

	Particle size (nm)	**PDI**	**Zeta potential (mV)**
Empty PPL	232.3 ± 2.97	0.20 ± 0.04	-9.9 ± 0.7
Dox-PPL	260.1 ± 4.63	0.19 ± 0.03	-36.1 ± 3.7
Empty HFB4L	233.1 ± 3.29	0.20 ± 0.01	-40.9 ± 0.3
Dox-HFB4L	253.4 ± 8.33	0.19 ± 0.02	-41.6 ± 1.6
Dox-PPL (-Sucrose)	252.6 ± 0.31	0.16 ± 0.07	-34.8± 5.8
Dox-HFB4L (-Sucrose)	253.0 ± 14.11	0.18 ± 0.05	-42.7 ± 2.1

TEM visuals of empty and Dox loaded formulations Dox- HFB4L and Dox-PPL are given in Figure 3. TEM images indicate that all generated liposomes have homogenous and spherical morphology (Figure 8). The Dox loaded liposomes have darker core parts, because of the drug loading (Figures 8B and 8D), and the empty liposomes on the contrary have light gray core parts (Figures 8A and 8C). TEM imaging is carried out under vacuum conditions, which may cause aqueous part in the liposomes' core to evaporate, leading to shrinkage. Consequently, the dimensions of the particles observed in TEM images may appear more compact than the values measured by dynamic light scattering (DLS) (55, 56).

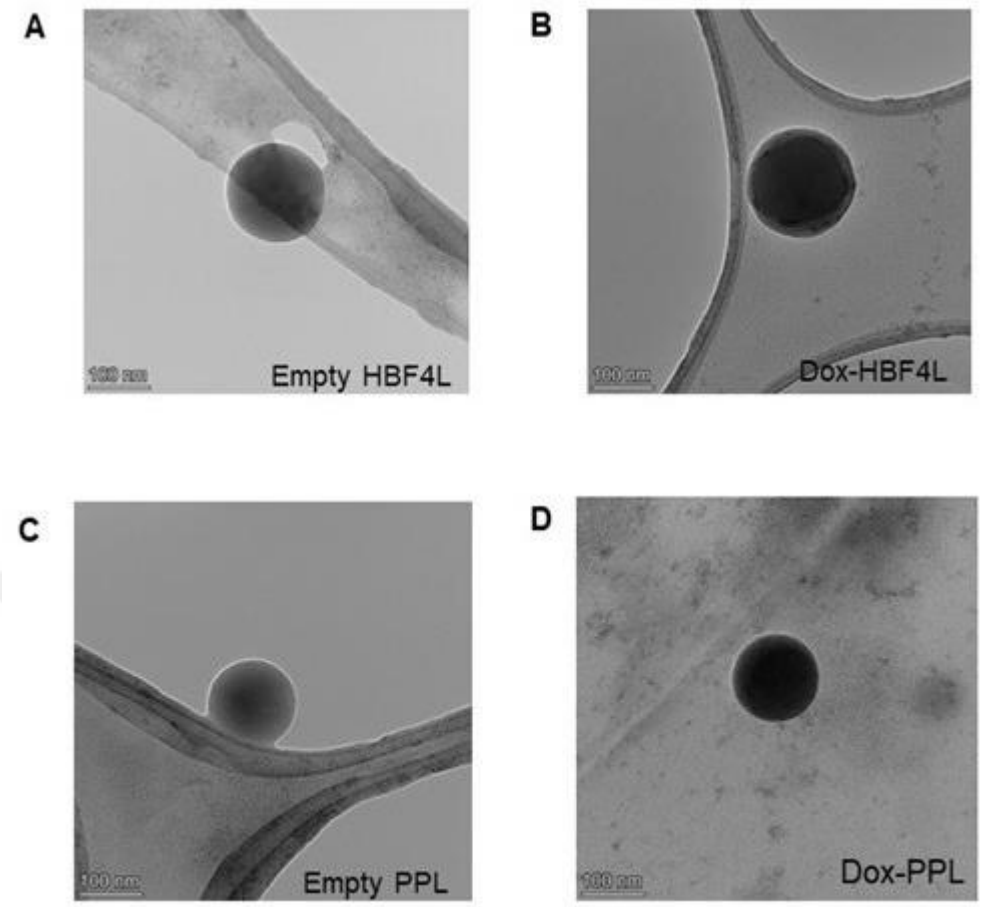

Figure 8. TEM images of HFB4L and PPL. Empty HFB4L (A) Dox-HFB4L (B) Empty PPL (C) Dox-PPL (D).

4.4 Stability of Dox-HFB4L and Dox-PPL

In PPL, Dox efficiency of encapsulation was determined as 20.9 % and in HFB4L Dox efficiency of encapsulation was calculated as 8.2 %. The encapsulation efficiencies of both forms were sufficient to complete this study, but further work has to be done to improve the encapsulation efficiency of formulations.

Sucrose was added for the long-term stability with the molar ratio 3:1(sucrose-to-lipid) before lyophilization of Dox liposomes. The existence of lyoprotectant also contributed to the re-solubilization of freeze-dried Dox loaded liposomes. Lyophilized liposomes were dissolved in water by manually mixing t20 s to protect them against drug leakage and then size and zeta potential assessments were made with DLS. The temporal change in particle size (Figure 9A), PDI (Figure 9B), and zeta potential

(Figure 4C) were determined at 4 °C (Figure 9). It is observed that the particle size (Figure 9A), PDI (Figure 9B), and zeta potential (Figure 9C) of liposomes statistically don't change over 60 days, which shows the stability of the Dox-HFB4L and Dox-PPL formulations.

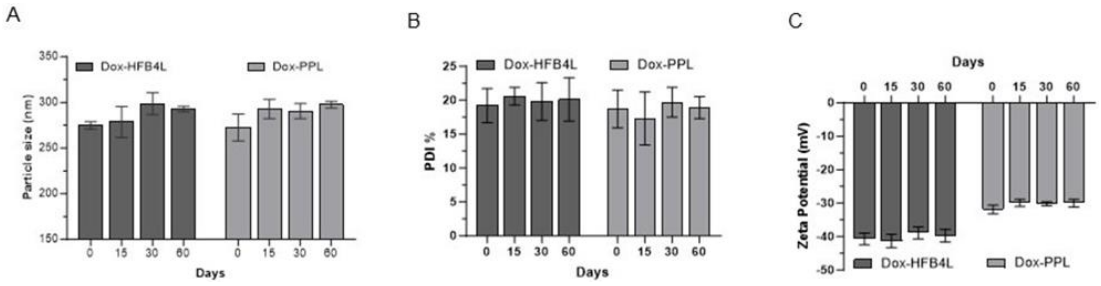

Figure 9. Stability of Dox-PPL and Dox-HFB4L for 60 days. Particle size (A), PDI (B), zeta potential (C).

Class I (4, 17-21) and Class II (5, 10) HFBs were utilized either for packaging the drug-loaded nanoparticles or covering the drug directly. In the study targeting curcumin delivery, the covering of just curcumin with HGFI performed superior steadiness than liquid HFBI for 96 h (20). But the long-term stability of new drug formulations with HFBs were not studied under the scope of these studies. It is known that liposomes face stability problems during storage, and this restricts their possible use as drug carrying agents. Both HFB4 and PEG coated liposomal formulations in this study show long-term stability at 4 °C for 60 days. Lyophilization to support the long-term stability was applied before in liposomal formulations (57). Sucrose and trehalose are known as powerful lyoprotectants to keep the unity of liposomes during lyophilization and then rehydration (52). In this study it is observed that the Dox-HFB4L in liquid form tended to aggregate after 72 h even storing at 4 °C. The measurements show that liposomes reach approximately 2.5-fold of their original size after 72 h. Gentle shaking to avoid drug leakage was useless to remove the aggregates. Aggressive vortexing on the other hand may cause drug leakage. For this reason, adding sucrose as a lyoprotectant with a stoichiometric ratio of 3:1 (sugar: lipid) prior to lyophilization solved this problem and adapted the formulation to a stable form for 2 months.

4.5 In vitro Dox Release from Dox-HFB4L and Dox-PPL

The drug release from Dox containing liposomes were presented time dependently at 37 ºC at physiological pH 7.4 and at acidic pH 5.6, same as the pH of the tumor tissue (58, 59). Both Dox loaded liposomal formulations showed 30% of drug release in the initial 4 h, with similar release scheme (Figure 10). Both Dox loaded liposomes released more drug at pH 5.6 with respect to pH 7.4, as presented in Figure 5 ($p<0.05$). This pattern is not affected by the storage of lyophilized formulations at 4 °C for 60 days (Figure 10).

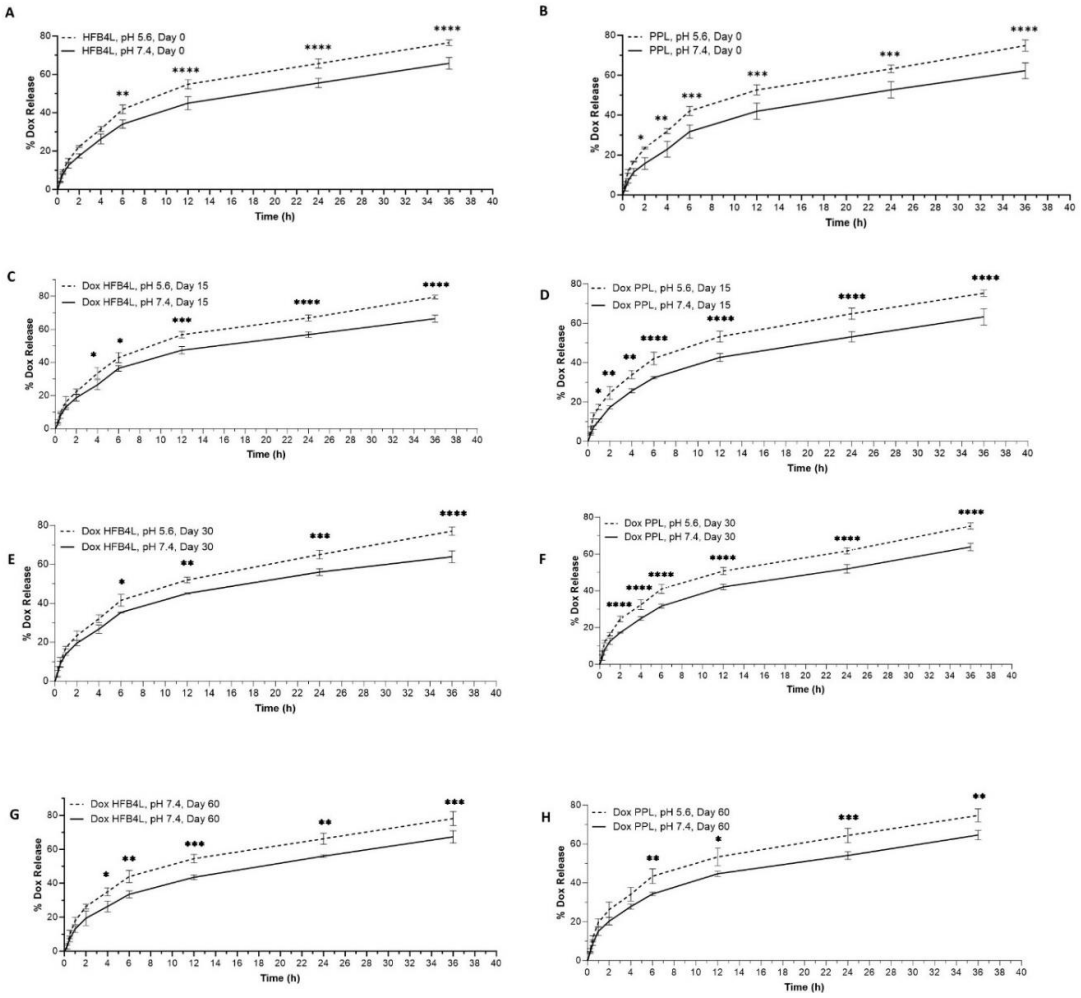

Figure 10. Release profiles of Dox-HFB4L (A, C, E, G) and Dox-PPL (B, D, F, H) for pH 5.6 and pH 7.4 by time.

The drug released from both Dox loaded liposomes was statistically higher at acidic pH with respect to physiological pH 7.4. This property may offer an advantage

in delivering more drug to the tumor environment. Barani et al studied delivering Dox encapsulated in Class II HFB1 coated niasome and showed that the new formulation released more Dox in an acidic pH (5). In this study, Dox release from both liposomal formulations remained consistent over a period of two months at various pH levels. Release studies performed with Class I HFBs showed no distinction in Dox release at pH 7.4 and pH 5.5 (4, 19). This is due to the superior stability of Class I HFBs, as Class I rHGFI retains its biological activity even under extreme pH levels (19). Class I HFB proteins can self-assemble into rodlets, morphologically a resilient fibrillar structure. The class II HFBs on the other hand, can self-assemble but lacking this fibrillar morphology (20). As a result, Class II HFB4 may be used as an alternative to PEG liposomes, since they may provide superior benefit for bringing hydrophobic agents to acidic tumor tissues and cells.

4.6 Cellular Uptake and Cytotoxicity of free Dox, Dox-HFB4L, and Dox-PPL in MCF7 cells

Internalization of free Dox, Dox loaded liposomes into the MCF7 cells is presented with the flow cytometry histogram. The red and blue right shift of the fluorescence intensity in Figure 6 indicated that Dox in three formulations were taken into the MCF7 cells. Treatment with 5 μM Dox-HFB4L, and 5 μM Dox-PPL generate elevated average fluorescent intensity (MFI) with respect to 5 μM free Dox (Figure 11 C). There was no significant MFI difference between two Dox loaded liposomal formulations (Figure 11). These outputs indicate that liposomal formulations have resembling and improved cellular uptake with respect to free Dox.

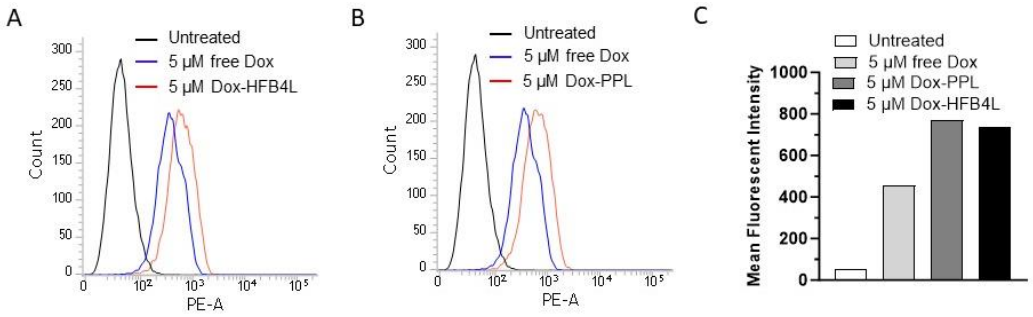

Figure 11. Cellular uptake results for free Dox, Dox PPL, and Dox-HFB4L. Flow cytometry analysis results of MCF7 cells with incubation 5 µM of free Dox (blue), and untreated cells (black), Dox-HFB4L (red) (A). Flow cytometry analysis results of MCF7 cells with incubation 5 µM of free Dox (blue), untreated cells (black), and Dox-PPL (red) (B). Mean fluorescent intensity after treatment of MCF7 cells with 5 µM of free Dox, Dox PPL and Dox-HFB4L (C).

At first, the effect of HFB4 on cell growth was tested with MCF7 cell line to find the nontoxic amount of HFB4. HFB4s half-maximum inhibitory concentration (IC50) was calculated as 62.40 µM at 72 h (R^2= 0.99) (Figure 12A).

Then, the nontoxic concentration of HFB4 0.4 µM was tested and it is seen that this concentration had no considerable effect on MCF7 cell growth in the liposomal formulations (Figure 12A). The cellular toxicity and IC50 values of free Dox, liposomal Dox on MCF7 cells is presented in Figure 7.

IC50 values after 72 h exposure to free Dox and liposomal Dox formulations were calculated as 0.35 µM (Figure 12B), 0.59 µM (Figure 12D), and 0.46 µM (Figure 12C). The half-maximum inhibitory concentration of Dox-HFB4L was 1.28 times lower than free Dox-PPL (Figures 12C and12 D). However, half-maximum inhibitory concentration of Dox-HFB4L was 1.32 times higher than free Dox (Figures 12B and 12C), and IC50 values of Dox-PPL was 1.67 times higher than free Dox (Figures 12B and 12D).

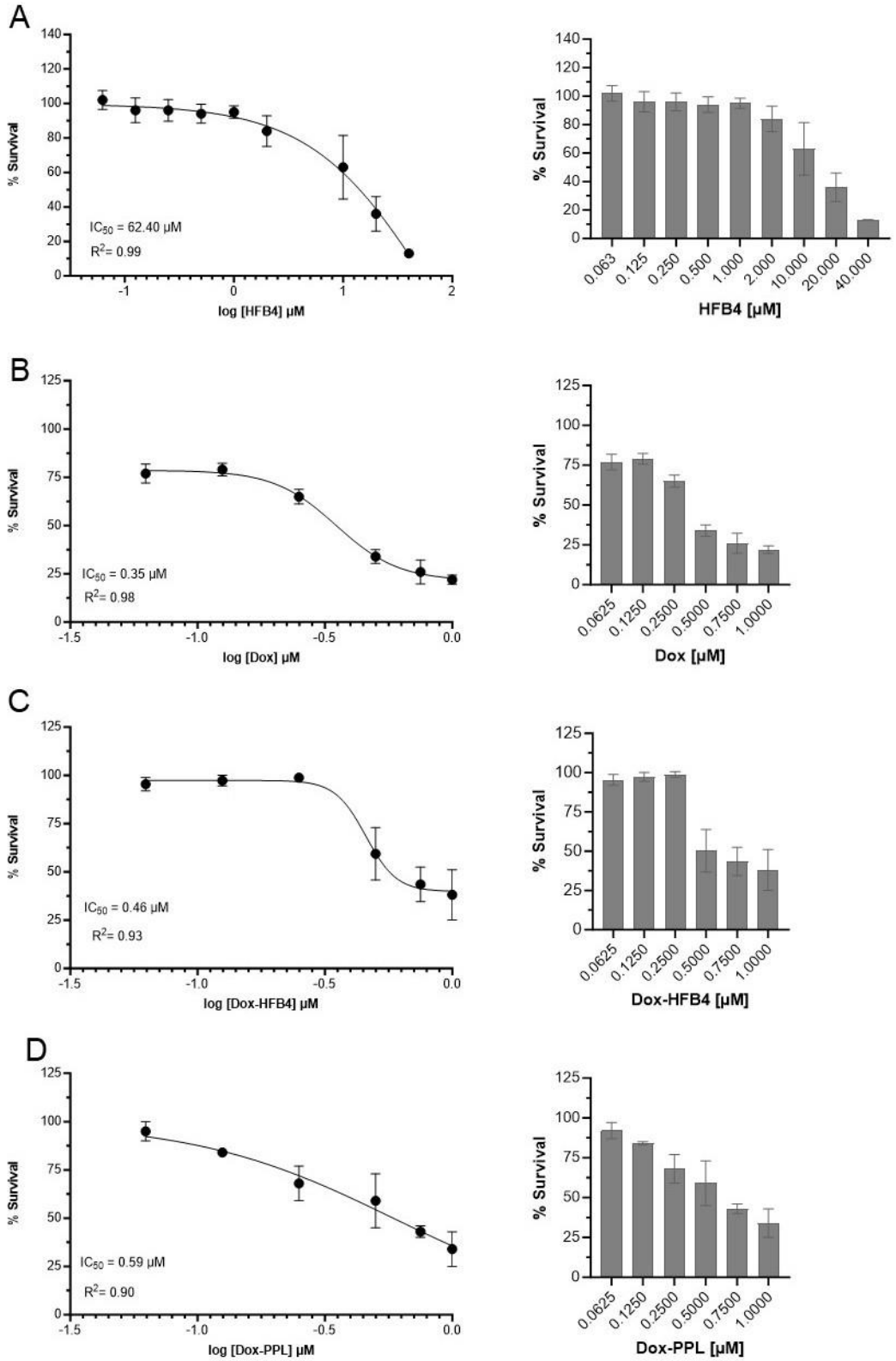

Figure 12. The IC50 of HFB4 in MCF7 cells, 72 h (A), Dox (B), Dox-PPL (C), Dox-HFB4L (D). Percent survival was presented with bar graphs.

Both liposomal Dox forms present improved internalization to cells with respect to free Dox, however they offer reduced antitumor effect because of the prolonged release of the drug. This result is in line with the study investigating the anticancer effect of the HFB1 coated or PEG coated niasome (5). Notably, Dox-HFB4L cytotoxicity is higher in MCF7 cells than Dox-PPL.

5 DISCUSSION

Liposomes are widely studied as a drug distribution method owing to their biocompatibility, biodegradability and capability to carry both water-soluble and water-dissoluble drugs. They also provide an alternative for increasing bioavailability of poorly soluble drugs.

Although liposomes have many advantages, there are also some weaknesses such as instability, limited shelf life, low encapsulation efficiency and quick elimination from blood circulation by reticulo-endothelial system (29). So, efforts for improved drug delivery are focusing on these weaknesses. The newly produced HFB4 coated liposome targets a stable formulation with a favorable particle characteristic, prolonged stay in circulation by evading from immune system and improved therapeutic effect.

Tumor and inflammatory tissues are distinguished by enhanced vascular permeability. This phenomenon is linked to malignant tissues, which form a discontinuous endothelium with large vascular fenestrations (pores). These fenestrations enable liposomes smaller than approximately 500 nm to diffuse out of the blood vessels (extravasation) and access the tumor interstitial space (60). This study present that generated Dox liposomes reach nanomeric size around 250 nm with a low PDI index and may allow extravasation of drug-loaded liposomes at the tumor site.

Only other study combining Dox with HFB coating is in niasome formulation (5). In that study generated niasome size was 593 nm with 0.27 PDI index at pH 7.4. The size of Dox-HFB4L generated in thesis study is less than 500 nm, meeting the extravasation criteria, and smaller than the HFB niasomal formulation.

Even smaller sized nanocarriers were produced targeting other chemicals. Studies on curcumin in HFB coated PLGA nanocarrier generated 144 nm drug carrying particles (4). Direct coating of curcumin with HFB (19) generated 193 nm

nanoparticles. Direct coating of another anti-cancer drug docetaxel with HFB (18) generated nanocarrier between 303.7- 185.6 nm size with a narrow PDI index.

A key indicator of instability is particle aggregation, which occurs when particles exhibit a stronger attraction to each other than to solvent molecules. Consequently, zeta potential—a measure of the electric potential at the particle's outer layer at the slip plane—is often used to assess liposome stability (61). For a stable nanosuspension relying on electrostatic repulsion, zeta potential of ±30 mV and beyond is accepted as necessary. High negative zeta potential values, which inhibit aggregation, indicate stable formulations.(5). For instance, liposomes with very low zeta potential around -80 mV, often resulting from high ionization of functional groups like carboxyl groups, are considered highly stable. (61).

In the study results, it is observed that introduction of Dox to liposomes decreases zeta potential. Also, HFB4 liposomes have lower zeta potential than PEG liposomes, which indicates higher stability. Similar results was found in HFB coated Dox niasome study (5), such that addition of Dox to bare niasome decreased the zeta potential. Also, at pH 7.4 HFB coated Dox niasome has lower zeta potential than PEG coated Dox niasome in line with the study results. In only study carried out with HFBIV (6), coating of transferrin fused porous silicon nanoparticle (PSi NP + Tf) with HFBIV (PSi NP + Tf-HFBIV) decreased the zeta potential approximately by -8 mV, which is similar to this study results. Either with direct drug coating or with NP coating, a negative zeta potential was observed in formulations with utilizing HFB (4-6, 18, 19).

Passive or active loading method can be utilized to upload the lipophilic drug Dox into liposomes. In this study the most commonly used passive loading method, the thin-film hydration method, was selected for drug encapsulation. The Dox solution was incorporated into the phospholipids prior to film formation, allowing the hydrophobic Dox to passively partition and accumulate within the liposome shells. It is known that the simplicity of this method was compromised with small drug encapsulation percentages. In contrast, active methods, also referred to as remote

loading techniques, utilize pH gradients between the blank liposome's acidic core buffer and the Dox containing external buffer Dox. Under neutral conditions, the drug molecules present with the formed liposomes can permeate selectively via the lipids transmembrane. The available form of liposomal Dox in the market, Myocet®, is utilized this approach and the drug entrapment efficiencies is greater than 95% (62). Drug encapsulation efficiency in this study can be improved by changing the loading method of Dox from passive to active loading.

Stability study started with liquid forms of Dox-HFB4L, Dox-PPL but at day three measurement of hydrodynamic diameter indicated 150% particle size increase compared to day zero for Dox-HFB4L. For this reason, a freeze-drying process was applied for long-term storage and to evaluate the stability. It is known that freezing and freeze-drying affect liposome stability so there is a need for lyoprotectant to preserve liposome stability. For lyophilization, disaccharides like sucrose or trehalose are considered to be the most efficient lyoprotectants, due to their high viscosity, low molecular flexibility after drying and ability to generate an amorphous, glass matrix (52). In this study sucrose with a molar ratio 3:1 (sugar:lipid) before lyophilization was applied based on the study that 2.3 (sucrose: lipid) molar ratio and above, the difference in average particle size of liposomes before and after lyophilization seems negligible (49).

Studies regarding direct drug coating or drug loaded NP coating with HFB don't provide any long-term data on drug stability at any storage conditions. In direct covering of curcumin with Class I HFB indicated superior stability than Class II HFB kept in aquous form after 96 h (20). In another study, direct covering of curcumin with the same Class I HFB, the produced drug nanocarrier was vacuum freeze-dried. Characterization studies were done by dissolving the freeze-dried powder but there was no information about time dependent change of size and zeta potential of nanocarrier (19). In coating curcumin loaded PLGA NP with Class I HFB study, again produced HFB coated NP's were lyophilized and drug loading was measured with dissolving the lyophilized form (4). There was no information about the storage conditions and long-term results on stability in this study. In other studies (5, 18)

results were based on liquid nanocarrier formulation, in which long term stability was not under the scope of the experiments. However, instability of liposomes at shelf is the major limiting point for their use for drug delivery. This study is unique in terms of providing long term stability results for 60 days, with application of an appropriate cryoprotectant while lyophilization.

In the study, the release profile of both liposomal formulations doesn't change by time. In both Dox loaded liposome formulations, drug release at pH 5.6 was higher than the drug release at pH 7.4. Difference at release rates at different pH become statistically significant starting from 6 h. There is no burst release in the initial period, such that only 25 % of Dox was discharged after 4 h at pH 7.4. On the other hand, at pH 5.6, the release rates were higher around 30 % at 4 h. These values are far below the 100 % of free Dox release obtained at pH 7.4 after 4 h (5). This study shows a pH sensitive release of Dox, in parallel with Class II HFB HFB1 coated niasome study (5). On the contrary, release studies done with Class I HFBs don't indicate any distinction in discharge rates at different pH (4, 19). The resemblance in release percentages at different pH levels was accredited to steadiness of Class I HFBs, which allows Class I HFB rHGFI to maintain its biological activity even under extreme pH conditions (19). In terms of configuration, Class I HFB can self-assemble to a chemically resilient fibrillar form which are rodlets. On the contrary, the class II HFB self-assemble to an extended network without any fibrillar framework (20). So, it can be concluded that the HFB4 coating secures Dox to cross slower from the layers of liposome and ensure a controlled release. Also due to its class characteristics it may be more sensitive to pH. It is known that tumor cells generate acid for this reason their intracellular pH is approximately 5.5. So, an increased release rate in acidic pH may offer a benefit treatment with Dox-HFB4L.

The flow cytometry studies show superior cellular uptake profiles for both Dox loaded liposomes with respect to to free Dox, but higher cytotoxicity was obtained with free Dox. IC50 of free Dox was 0.35 μM, whereas Dox-HFB4L IC50 value was 0.46 μM, 31 % higher than free Dox. IC50 of Dox-PPL is even 69 % higher than free Dox with 0.59 μM concentration. This may be attributed to rapid release of free Dox

versus the controlled release of liposomal formulations, such that only 60 % of the total drug was released after 36 h at pH 7.4. This may affect the cytotoxicity results obtained after 72 h incubation of cells with different Dox formulations. However, the difference in cytotoxicity between Dox-HFB4L and Dox-PPL cannot be explained with these parameters since the drug release and cellular uptake profiles of two formulations were similar. Dox-HFB4L has superior toxic effect on cancer cells than Dox-PPL at the same concentration.

6 CONCLUSION

This study characterized and assessed antitumor activity of class II, HFB4-coated empty, and Dox-loaded liposomes and compared them with PEGylated liposomes. The HFB4 envelop enhanced the steadiness of Dox-HFB4L for two months in lyophilized form at 4 °C without altering drug release from HFB4L. The new formulation also promoted greater Dox discharge at low pH with respect to physiological pH. Resembling features were noticed in Dox-PPL. Although both forms demonstrated enhanced cellular internalization with respect to free Dox, they show a reduced antitumor activity due to the prolonged release of Dox. Importantly, in MCF7 cell line Dox-HFB4L showed superior toxic effect compared to Dox-PPL in breast cancer cell line. Lastly, this study demonstrated that coating liposomes with HFB4 provides significant advantages in terms of stability, non-toxicity, and sustained delivery of hydrophobic drugs to the acidic tumor tissues and cells. However, further research is needed to enhance the encapsulation efficiency and explore in vivo efficacy of this new formulation.

7 REFERENCES

1. Singh BN, Singh BR, Gupta VK, Kharwar RN, Pecoraro L. Coating with Microbial Hydrophobins: A Novel Approach to Develop Smart Drug Nanoparticles. Trends Biotechnol. 2018;36(11):1103-6.
2. Jain A, Singh SK, Arya SK, Kundu SC, Kapoor S. Protein Nanoparticles: Promising Platforms for Drug Delivery Applications. ACS Biomaterials Science & Engineering. 2018;4(12):3939-61.
3. Fam SY, Chee CF, Yong CY, Ho KL, Mariatulqabtiah AR, Tan WS. Stealth coating of nanoparticles in drug-delivery systems. Nanomaterials. 2020;10(4):787.
4. Sun L, Xu H, Xu J-h, Wang S-n, Wang J-w, Zhang H-f, et al. Enhanced Antitumor Efficacy of Curcumin-Loaded PLGA Nanoparticles Coated with Unique Fungal Hydrophobin. AAPS PharmSciTech. 2020;21:1-10.
5. Barani M, Mirzaei M, Torkzadeh-Mahani M, Lohrasbi-Nejad A, Nematollahi MH. A new formulation of hydrophobin-coated niosome as a drug carrier to cancer cells. Materials Science and Engineering: C. 2020;113:110975.
6. Reuter LJ, Shahbazi MA, Mäkilä EM, Salonen JJ, Saberianfar R, Menassa R, et al. Coating Nanoparticles with Plant-Produced Transferrin-Hydrophobin Fusion Protein Enhances Their Uptake in Cancer Cells. Bioconjug Chem. 2017;28(6):1639-48.
7. Maiolo D, Pigliacelli C, Sánchez Moreno P, Violatto MB, Talamini L, Tirotta I, et al. Bioreducible Hydrophobin-Stabilized Supraparticles for Selective Intracellular Release. ACS Nano. 2017;11(9):9413-23.
8. Taniguchi S, Sandiford L, Cooper M, Rosca EV, Ahmad Khanbeigi R, Fairclough SM, et al. Hydrophobin-Encapsulated Quantum Dots. ACS Applied Materials & Interfaces. 2016;8(7):4887-93.
9. Wösten HA, Scholtmeijer K. Applications of hydrophobins: current state and perspectives. Applied microbiology and biotechnology. 2015;99:1587-97.
10. Valo HK, Laaksonen PH, Peltonen LJ, Linder MB, Hirvonen JT, Laaksonen TJ. Multifunctional hydrophobin: toward functional coatings for drug nanoparticles. Acs Nano. 2010;4(3):1750-8.
11. Espino-Rammer L, Ribitsch D, Przylucka A, Marold A, Greimel KJ, Herrero Acero E, et al. Two novel class II hydrophobins from Trichoderma spp. stimulate enzymatic hydrolysis of poly(ethylene terephthalate) when expressed as fusion proteins. Appl Environ Microbiol. 2013;79(14):4230-8.
12. von Vacano B, Xu R, Hirth S, Herzenstiel I, Rückel M, Subkowski T, Baus U. Hydrophobin can prevent secondary protein adsorption on hydrophobic substrates without exchange. Analytical and bioanalytical chemistry. 2011;400:2031-40.

13. Sarparanta M, Bimbo LM, Rytkönen J, Mäkilä E, Laaksonen TJ, Laaksonen P, et al. Intravenous Delivery of Hydrophobin-Functionalized Porous Silicon Nanoparticles: Stability, Plasma Protein Adsorption and Biodistribution. Molecular Pharmaceutics. 2012;9(3):654-63.
14. Aimanianda V, Bayry J, Bozza S, Kniemeyer O, Perruccio K, Elluru SR, et al. Surface hydrophobin prevents immune recognition of airborne fungal spores. Nature. 2009;460(7259):1117-21.
15. Wang B, Han Z, Song B, Yu L, Ma Z, Xu H, Qiao M. Effective drug delivery system based on hydrophobin and halloysite clay nanotubes for sustained release of doxorubicin. Colloids and Surfaces A: Physicochemical and Engineering Aspects. 2021;628:127351.
16. Paslay LC, Falgout L, Savin DA, Heinhorst S, Cannon GC, Morgan SE. Kinetics and Control of Self-Assembly of ABH1 Hydrophobin from the Edible White Button Mushroom. Biomacromolecules. 2013;14(7):2283-93.
17. Akanbi MHJ, Post E, Meter-Arkema A, Rink R, Robillard GT, Wang X, et al. Use of hydrophobins in formulation of water insoluble drugs for oral administration. Colloids and surfaces B: Biointerfaces. 2010;75(2):526-31.
18. Fang G, Tang B, Liu Z, Gou J, Zhang Y, Xu H, Tang X. Novel hydrophobin-coated docetaxel nanoparticles for intravenous delivery: in vitro characteristics and in vivo performance. European Journal of Pharmaceutical Sciences. 2014;60:1-9.
19. Niu B, Li M, Jia J, Zhang C, Fan Y-Y, Li W. Hydrophobin-enhanced stability, dispersions and release of curcumin nanoparticles in water. Journal of Biomaterials Science, Polymer Edition. 2020;31(14):1793-805.
20. Song D, Wang X, Yang J, Ge L, Wang B, Xu H, et al. Hydrophobin HGFI improving the nanoparticle formation, stability and solubility of Curcumin. Colloids and Surfaces A: Physicochemical and Engineering Aspects. 2021;610:125922.
21. Han Z, Song B, Yang J, Wang B, Ma Z, Yu L, et al. Curcumin-Encapsulated Fusion Protein-Based Nanocarrier Demonstrated Highly Efficient Epidermal Growth Factor Receptor-Targeted Treatment of Colorectal Cancer. J Agric Food Chem. 2022;70(49):15464-73.
22. Tahover E, Patil YP, Gabizon AA. Emerging delivery systems to reduce doxorubicin cardiotoxicity and improve therapeutic index: focus on liposomes. Anticancer Drugs. 2015;26(3):241-58.
23. Senapati S, Mahanta AK, Kumar S, Maiti P. Controlled drug delivery vehicles for cancer treatment and their performance. Signal transduction and targeted therapy. 2018;3(1):7.
24. Schöttler S, Becker G, Winzen S, Steinbach T, Mohr K, Landfester K, et al. Protein adsorption is required for stealth effect of poly(ethylene glycol)- and poly(phosphoester)-coated nanocarriers. Nature Nanotechnology. 2016;11(4):372-7.
25. Du H, Chandaroy P, Hui SW. Grafted poly-(ethylene glycol) on lipid surfaces inhibits protein adsorption and cell adhesion. Biochimica et Biophysica Acta (BBA) - Biomembranes. 1997;1326(2):236-48.

26. Hatakeyama H, Akita H, Harashima H. A multifunctional envelope type nano device (MEND) for gene delivery to tumours based on the EPR effect: A strategy for overcoming the PEG dilemma. Advanced Drug Delivery Reviews. 2011;63(3):152-60.
27. Abouelmagd SA, Sun B, Chang AC, Ku YJ, Yeo Y. Release kinetics study of poorly water-soluble drugs from nanoparticles: are we doing it right? Molecular pharmaceutics. 2015;12(3):997-1003.
28. Chen E, Chen B-M, Su Y-C, Chang Y-C, Cheng T-L, Barenholz Y, Roffler SR. Premature Drug Release from Polyethylene Glycol (PEG)-Coated Liposomal Doxorubicin via Formation of the Membrane Attack Complex. ACS Nano. 2020;14(7):7808-22.
29. Yadav D, Sandeep K, Pandey D, Dutta RK. Liposomes for Drug Delivery. Journal of biotechnology & biomaterials. 2017;2017:1-8.
30. Kalepu S, Nekkanti V. Insoluble drug delivery strategies: review of recent advances and business prospects. Acta Pharmaceutica Sinica B. 2015;5(5):442-53.
31. Hektor HJ, Scholtmeijer K. Hydrophobins: proteins with potential. Current Opinion in Biotechnology. 2005;16(4):434-9.
32. Rivankar S. An overview of doxorubicin formulations in cancer therapy. J Cancer Res Ther. 2014;10(4):853-8.
33. Park JH, Lee S, Kim J-H, Park K, Kim K, Kwon IC. Polymeric nanomedicine for cancer therapy. Progress in polymer science. 2008;33(1):113-37.
34. Parveen S, Sahoo SK. Polymeric nanoparticles for cancer therapy. Journal of drug targeting. 2008;16(2):108-23.
35. Mitra S, Gaur U, Ghosh PC, Maitra AN. Tumour targeted delivery of encapsulated dextran-doxorubicin conjugate using chitosan nanoparticles as carrier. J Control Release. 2001;74(1-3):317-23.
36. Elzoghby AO, Samy WM, Elgindy NA. Albumin-based nanoparticles as potential controlled release drug delivery systems. J Control Release. 2012;157(2):168-82.
37. Dreis S, Rothweiler F, Michaelis M, Cinatl J, Jr., Kreuter J, Langer K. Preparation, characterisation and maintenance of drug efficacy of doxorubicin-loaded human serum albumin (HSA) nanoparticles. Int J Pharm. 2007;341(1-2):207-14.
38. Jin X, Zhang P, Luo L, Cheng H, Li Y, Du T, et al. Efficient intravesical therapy of bladder cancer with cationic doxorubicin nanoassemblies. Int J Nanomedicine. 2016;11:4535-44.
39. Wei T, Chen C, Liu J, Liu C, Posocco P, Liu X, et al. Anticancer drug nanomicelles formed by self-assembling amphiphilic dendrimer to combat cancer drug resistance. Proc Natl Acad Sci U S A. 2015;112(10):2978-83.
40. Yu G, Zhao R, Wu D, Zhang F, Shao L, Zhou J, et al. Pillar[5]arene-based amphiphilic supramolecular brush copolymer: fabrication, controllable self-assembly and application in self-imaging targeted drug delivery. Polym Chem. 2016;7(40):6178-88.
41. Lin CC, Metters AT. Hydrogels in controlled release formulations: network design and mathematical modeling. Adv Drug Deliv Rev. 2006;58(12-13):1379-408.

42. Xue B, Kozlovskaya V, Liu F, Chen J, Williams JF, Campos-Gomez J, et al. Intracellular Degradable Hydrogel Cubes and Spheres for Anti-Cancer Drug Delivery. ACS Appl Mater Interfaces. 2015;7(24):13633-44.
43. Wang Y, Nie J, Chang B, Sun Y, Yang W. Poly(vinylcaprolactam)-based biodegradable multiresponsive microgels for drug delivery. Biomacromolecules. 2013;14(9):3034-46.
44. Yu J, Ha W, Sun JN, Shi YP. Supramolecular hybrid hydrogel based on host-guest interaction and its application in drug delivery. ACS Appl Mater Interfaces. 2014;6(22):19544-51.
45. Gasteiger E, Hoogland C, Gattiker A, Duvaud Se, Wilkins MR, Appel RD, Bairoch A. Protein identification and analysis tools on the ExPASy server: Springer; 2005.
46. Madeira F, Pearce M, Tivey ARN, Basutkar P, Lee J, Edbali O, et al. Search and sequence analysis tools services from EMBL-EBI in 2022. Nucleic Acids Res. 2022;50(W1):W276-W9.
47. Lin-Cereghino J, Lin-Cereghino G. Vectors and Strains for Expression. Methods in molecular biology (Clifton, NJ). 2007;389:11-26.
48. Cai F, Gao R, Zhao Z, Ding M, Jiang S, Yagtu C, et al. Evolutionary compromises in fungal fitness: hydrophobins can hinder the adverse dispersal of conidiospores and challenge their survival. The ISME Journal. 2020;14(10):2610-24.
49. Yang T, Cui F-D, Choi M-K, Lin H, Chung S-J, Shim C-K, Kim D-D. Liposome formulation of paclitaxel with enhanced solubility and stability. Drug delivery. 2007;14(5):301-8.
50. Franzé S, Selmin F, Samaritani E, Minghetti P, Cilurzo F. Lyophilization of liposomal formulations: still necessary, still challenging. Pharmaceutics. 2018;10(3):139.
51. Sonju JJ, Shrestha P, Dahal A, Gu X, Johnson WD, Zhang D, et al. Lyophilized liposomal formulation of a peptidomimetic-Dox conjugate for HER2 positive breast and lung cancer. International Journal of Pharmaceutics. 2023;639:122950.
52. Stark B, Pabst G, Prassl R. Long-term stability of sterically stabilized liposomes by freezing and freeze-drying: Effects of cryoprotectants on structure. European journal of pharmaceutical sciences. 2010;41(3-4):546-55.
53. Przylucka A, Akcapinar GB, Bonazza K, Mello-de-Sousa TM, Mach-Aigner AR, Lobanov V, et al. Comparative Physiochemical Analysis of Hydrophobins Produced in Escherichia Coli and Pichia Pastoris. Colloids and Surfaces B: Biointerfaces. 2017;159:913-23.
54. Soema PC, Willems G-J, Jiskoot W, Amorij J-P, Kersten GF. Predicting the influence of liposomal lipid composition on liposome size, zeta potential and liposome-induced dendritic cell maturation using a design of experiments approach. European Journal of Pharmaceutics and Biopharmaceutics. 2015;94:427-35.
55. Mohan A, Narayanan S, Sethuraman S, Krishnan UM. Novel resveratrol and 5-fluorouracil coencapsulated in PEGylated nanoliposomes improve chemotherapeutic efficacy of combination against head and neck squamous cell carcinoma. Biomed Res Int. 2014;2014:424239.

56. Monnier C, Thévenaz D, Balog S, Fiore G, Vanhecke D, Rothen-Rutishauser B, Fink A. A guide to investigating colloidal nanoparticles by cryogenic transmission electron microscopy: Pitfalls and benefits. AIMS Biophysics. 2015;2:245-58.
57. van Winden ECA, Crommelin DJA. Long term stability of freeze-dried, lyoprotected doxorubicin liposomes. European Journal of Pharmaceutics and Biopharmaceutics. 1997;43(3):295-307.
58. Liu J, Chen Q, Feng L, Liu Z. Nanomedicine for tumor microenvironment modulation and cancer treatment enhancement. Nano Today. 2018;21:55-73.
59. Boedtkjer E, Pedersen SF. The Acidic Tumor Microenvironment as a Driver of Cancer. Annual Review of Physiology. 2020;82(1):103-26.
60. Lombardo D, Calandra P, Barreca D, Magazù S, Kiselev MA. Soft Interaction in Liposome Nanocarriers for Therapeutic Drug Delivery. Nanomaterials. 2016;6(7):125.
61. Dymek M, Sikora E. Liposomes as biocompatible and smart delivery systems – the current state. Advances in Colloid and Interface Science. 2022;309:102757.
62. Ibrahim M, Abuwatfa WH, Awad NS, Sabouni R, Husseini GA. Encapsulation, Release, and Cytotoxicity of Doxorubicin Loaded in Liposomes, Micelles, and Metal-Organic Frameworks: A Review. Pharmaceutics. 2022;14(2).

8 CURRICULUM VITAE